

Diploma thesis



HTL1 Lastenstraße Klagenfurt, department of mechatronics  
Lastenstraße 1, 9020 Klagenfurt, Austria

# Digital 3D compass

for the degree of  
Ingenieur

by  
THOMAS GRUEBLER  
born 20 September 1991  
citizen of Villach - Austria

supervised by:  
Prof. DI Breithuber, HTL1  
Ing. Martin Orasch, Infineon

in cooperation with



Infineon Technologies Austria AG

2011

## Erklärung

Ich erkläre hiermit, dass ich die vorliegende Diplomarbeit selbstständig verfasst und noch nicht anderweitig zu Prüfungszwecken vorgelegt habe. Sämtliche benutzte Quellen und Hilfsmittel sind angegeben, wörtliche und sinngemäße Zitate sind als solche gekennzeichnet.

## Declaration

Hereby I assure, that I made the thesis at hand without third parties' help only with the specified sources and aids. All figures, which were gathered from the sources, were marked as such. This thesis, in same or similar form, has not been available to any audit authority yet.

---

*Place, Date*

*Thomas Grübler*

## Danksagung

An dieser Stelle möchte ich mich bei allen bedanken, welche mich bei dieser Arbeit unterstützt haben.

Herr Ing. Martin Orasch für die Ermöglichung dieser tollen Diplomarbeit.

Herr Prof. Dipl.-Ing. Raimund Breithuber für das perfekte Korrekturlesen.

Herr Dipl.-Ing. Bernhard Schaffer und Herr Dipl.-Ing. (FH) Wolfgang Granig welche mir einen Algorithmus für einfache digitale Filter zeigten.

Herr Prof. Dipl.-Ing. Michael Bodner für weiterführende Einführung in digitales Filterdesign mit MATLAB.

Klassenkamerade Herr Daniel Götzhaber für seine Unterstützung bei den Fotografien.

Meinen besonderen Dank spreche ich dem gesamtem Team der SC Abteilung aus, welches mich wunderbar in ihre Gemeinschaft aufnahm und mir immer hilfsbereit beiseite stand.

*We can't define anything precisely.*<sup>1</sup>

---

<sup>1</sup>Richard P. Feynman - The Feynman Lectures on Physics, Volume I, 8-2

## 0.1 Abstract

The challenge of this diploma thesis was to develop a digital 3D compass based on Infineon Technologies hall-sensors.

For this application the magnetic fields in X, Y and Z direction are each measured by a sensor. A 3D acceleration sensor detects (by measuring the earth gravity) the current tilt. Using both the values of the field and the acceleration sensors, a two-dimensional projection of a virtual compass needle is generated and showed on the display.

The thesis mainly consists of the electrical design including component selection, the development of the software and the construction of six end products for marketing.

The biggest challenge of the project was to filter and correct the output values of the hall sensors. The used hall-sensors are originally not developed for detecting low fields. The used type is currently used in the accelerator pedal, the throttle valve or the height regulation of Xenon headlamps in cars and withstands a temperature range from -40 bis 170°C.

The goal is to proof that today's automotive hall-sensor technology by Infineon is ready to measure low fields, even if it is not originally developed for this application.

## 0.2 Zusammenfassung

Aufgabe dieser Diplomarbeit war es, einen dreidimensionalen, digitalen Kompass auf Basis von Infineon Hall-Sensoren zu entwickeln.

Dazu werden die Magnetfelder in X, Y und Z Richtung mit je einem Sensor gemessen. Ein 3D Beschleunigungssensor erfasst (durch die Messung der Erdbeschleunigung) die Lage des Kompasses im Raum. Mit diesen Daten werden die 3 Felder verrechnet und dadurch eine zweidimensionale Projektion einer virtuellen Kompassnadel am Display erzeugt.

Die Arbeit besteht im Wesentlichen aus dem elektrischen Design inklusive Auswahl der Bauelemente, der Softwareentwicklung und dem Aufbau von sechs Endprodukten.

Die größte Herausforderung des Projekts war das Filtern und Korrigieren der Messwerte der Hall-Sensoren. Hall-Sensoren wurden ursprünglich dafür entwickelt, stärkere Magnetfelder zu messen. Der hier verwendete Typ findet derzeit Anwendung im Gaspedal, der Drosselklappe oder in der Höhenregulierung von XENON-Scheinwerfern in Autos und widersteht Temperaturen von -40 bis 170°C.

Ziel ist der Beweis, dass die heutige Hall-Sensor-Technologie bereits, auch wenn sie nicht dafür entwickelt wurde, zur Messung des Erdmagnetfeldes anwendbar wäre.

# Contents

|  |           |
|--|-----------|
| <b>Erklärung</b>                                 | <b>ii</b> |
| <b>Declaration</b>                               | <b>ii</b> |
| 0.1 Abstract . . . . .                           | v         |
| 0.2 Zusammenfassung . . . . .                    | vi        |
| <b>1 Introduction</b>                            | <b>1</b>  |
| <b>2 General</b>                                 | <b>2</b>  |
| 2.1 The earth magnetic field . . . . .           | 2         |
| 2.2 Magnetic field sensors . . . . .             | 3         |
| 2.2.1 The Infineon TLE4998 hall sensor . . . . . | 4         |
| 2.3 Acceleration sensor . . . . .                | 6         |
| 2.3.1 ADXL327 . . . . .                          | 6         |
| <b>3 Design-steps</b>                            | <b>8</b>  |
| 3.1 Design-step 1 - proof of concept . . . . .   | 8         |
| 3.1.1 Basic proof of concept . . . . .           | 8         |
| 3.1.2 Extended proof of concept . . . . .        | 8         |
| 3.2 Design-step 2 . . . . .                      | 9         |
| 3.3 Design-step 3 . . . . .                      | 10        |
| 3.4 Design-step 4 . . . . .                      | 11        |

|          |   |           |
|----------|---|-----------|
| <b>4</b> | <b>Hardware overview</b>                    | <b>12</b> |
| 4.1      | Sensors . . . . .                           | 12        |
| 4.2      | Display . . . . .                           | 14        |
| 4.3      | Microcontroller . . . . .                   | 14        |
| 4.4      | Battery . . . . .                           | 15        |
| <b>5</b> | <b>Magnetic field data correction</b>       | <b>16</b> |
| 5.1      | The raw data . . . . .                      | 16        |
| 5.2      | Filtering . . . . .                         | 17        |
| 5.3      | Calibration for offset correction . . . . . | 21        |
| <b>6</b> | <b>Accelerometer data correction</b>        | <b>22</b> |
| 6.1      | Filtering . . . . .                         | 22        |
| 6.1.1    | Analog lowpass filter . . . . .             | 22        |
| 6.1.2    | Digital lowpass filter . . . . .            | 22        |
| 6.2      | Offset correction . . . . .                 | 23        |
| <b>7</b> | <b>Angle calculation</b>                    | <b>25</b> |
| 7.1      | Basic . . . . .                             | 25        |
| 7.2      | 3D calculation . . . . .                    | 26        |
| 7.3      | Averaging . . . . .                         | 27        |
| <b>8</b> | <b>Power management</b>                     | <b>28</b> |
| 8.1      | Requirements . . . . .                      | 28        |
| 8.2      | Power supply . . . . .                      | 28        |
| 8.3      | LiPO batteries . . . . .                    | 29        |
| 8.3.1    | Overview . . . . .                          | 29        |
| 8.3.2    | Charger . . . . .                           | 30        |
| 8.3.3    | Protection . . . . .                        | 30        |
| 8.4      | Battery voltage measurement . . . . .       | 31        |

|           |                                 |           |
|-----------|---------------------------------|-----------|
| <b>9</b>  | <b>Software structure</b>       | <b>33</b> |
| <b>10</b> | <b>Conclusion and outlook</b>   | <b>37</b> |
| <b>A</b>  | <b>Schematics</b>               | <b>43</b> |
| <b>B</b>  | <b>PCB layout</b>               | <b>46</b> |
| <b>C</b>  | <b>Packaging</b>                | <b>48</b> |
| <b>D</b>  | <b>User manual</b>              | <b>51</b> |
| <b>E</b>  | <b>Sourcecode documentation</b> | <b>54</b> |
| <b>F</b>  | <b>Datasheets</b>               | <b>55</b> |

## Chapter 1

# Introduction

The project was launched to provide a demonstration object to Infineon Technologies Austria AG for showing the capabilities of modern hall-effect based sensors. The compass is using a TLE4998, a linear hall sensor for magnetic fields up to 200 mT. It is not officially promoted that this sensor is usable for low fields like the earth magnetic field with only about 40 – 50  $\mu\text{T}$ , but this project confirms what is possible with modern technology.



**Figure 1.1:** *Picture of the compass*

## Chapter 2

# General

## 2.1 The earth magnetic field

The total intensity of the magnetic field on the earth surface varies from  $24\mu\text{T}$  to  $66\mu\text{T}$  [8]. Figure 2.1 shows the field lines on the earth.

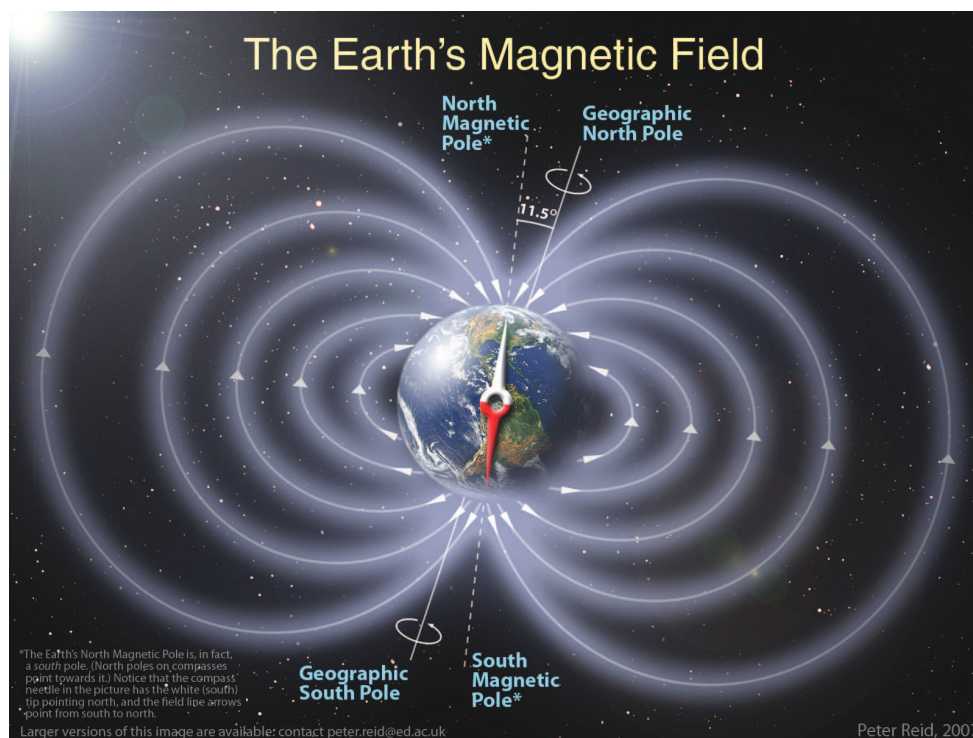
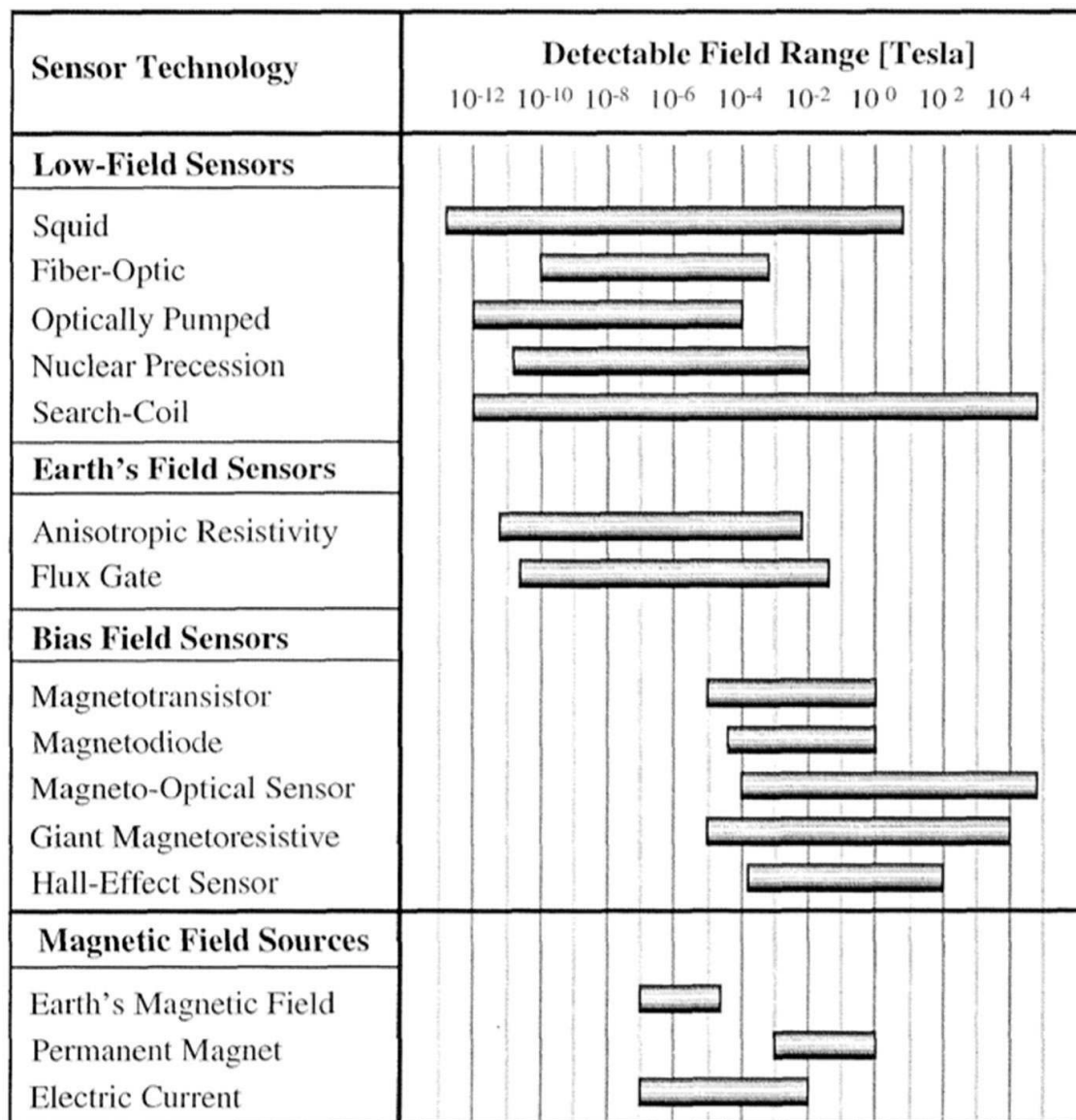


Figure 2.1: *Field lines on earth [7]*

## 2.2 Magnetic field sensors

There are several magnetic field sensors available. Figure 2.2 shows an overview of available methods to sense magnetic fields. Currently the most common automotive sensors are Hall-effect or GMR-effect based. Other effects like e.g. SQUIDs are mostly used for scientific applications.



**Figure 2.2:** Magnetic sensor technologies' and their detection capabilities. The sensors are divided in three different groups of field ranges: lowfield (nT), Earth's field ( $\mu$ T), and bias field (mT). [9]

### 2.2.1 The Infineon TLE4998 hall sensor

The TLE4998 is a programmable, linear, hall sensor for automotive usage. The main facts of the sensor are [5] :

- $V_{DD}$  : 4.5 – 5.5V
- $I_{DD}$  : 3.5 – 5.5mA
- Field range: 50, 100, 200mT (programmable)
- $f_{cutoff}$  of internal 1st order filter: 80 – 1390Hz (programmable)
- Interface: SENT, PWM, SPC

The detailed datasheet is appended.

#### Principle of operation

The main part of the sensor is a spinning-hall element for measuring the magnetig flux. "Spinning" means that the direction of the current through the hall plate and the direction of the hall voltage changes circular according to figure 2.3. The simplest form of it is just a changing polarity of the current through the hall plate. The DSP reads the hall voltage over an ADC and controls the "spin". This makes is possible to reduce the offsets caused by the hall probe and other parts.

Figure 2.4 describes the internal block diagram of the TLE4998S4. It also shows a temperature sensing unit to reduce linearity errors in analogue parts on high temperature changes (temperature range is -40 to 150°C) that occur in the automotive sector.

#### Communication interface

The sensor supports three main communication interfaces (SENT, PWM and SPC) and one proprietary programming interface [6]. Its documentation is appended. This interface is used in the project because it enables to read the raw hall\_adc data and other internal parameters.

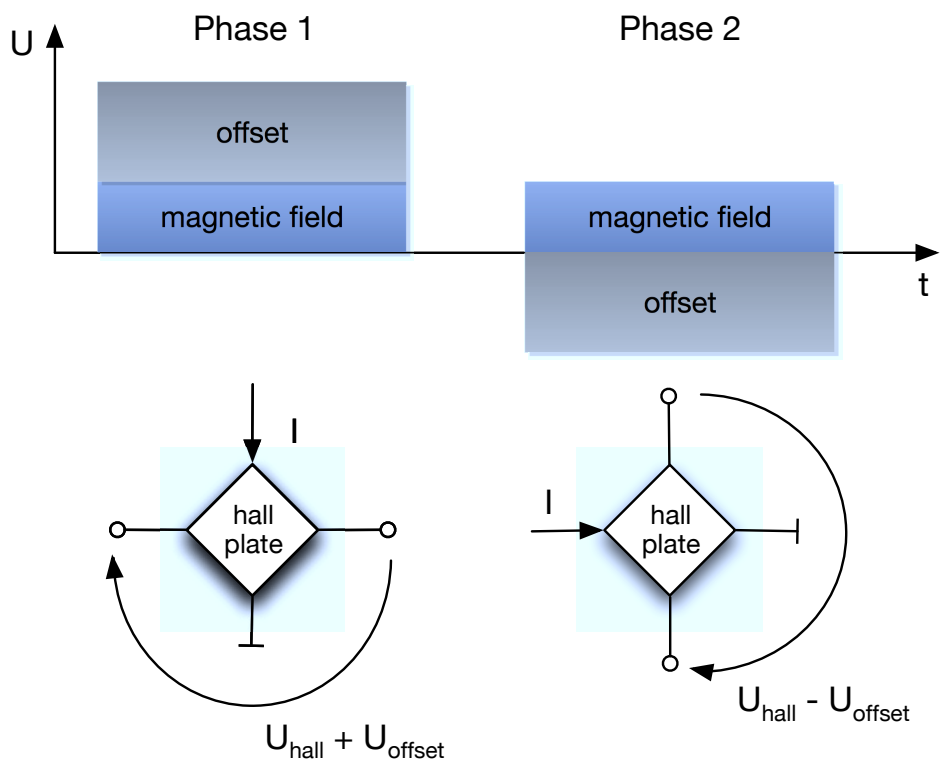


Figure 2.3: Functional principle of a spinning hall element, [4] modified

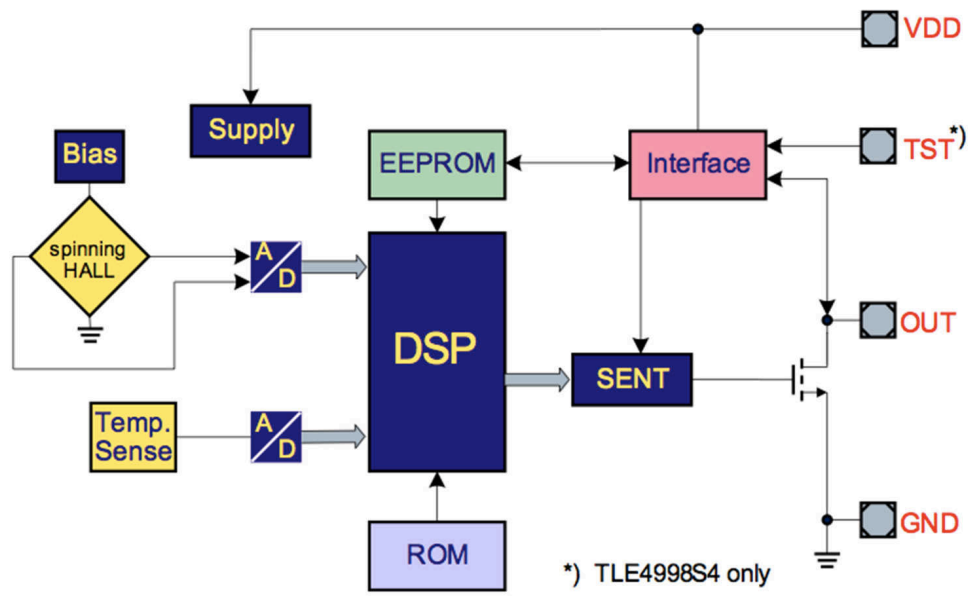


Figure 2.4: Block diagram [5]

## 2.3 Acceleration sensor

An acceleration sensor is used to measure the tilt of the device. This is needed to know in which direction the three magnetic field sensors are turned and so to find out, which sensors should be used for calculation of the angle to north.

### 2.3.1 ADXL327

Analog Devices ADXL327 [3] was the selected sensor. It has the following main specifications:

- 3-axis sensing
- measurement range : $\pm 2g$
- operating voltage:1.8 – 3.6V
- analog output with integrated bandwidth limiting by adding external capacitors

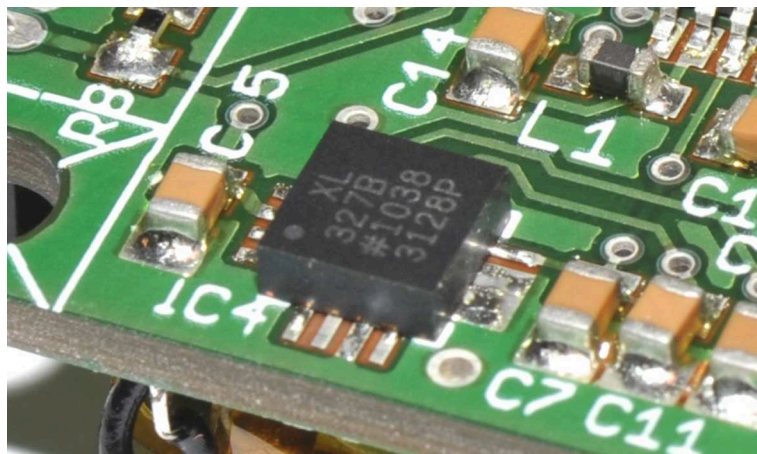


**Figure 2.5:** *Photograph of the mounted acceleration sensor*

#### Physical effect

*The ADXL327 is a complete 3-axis acceleration measurement system. The ADXL327 has a measurement range of  $\pm 2g$  minimum. It contains a polysilicon surface micromachined*

*sensor and signal conditioning circuitry to implement an open-loop acceleration measurement architecture. The output signals are analog voltages that are proportional to acceleration. The accelerometer can measure the static acceleration of gravity in tilt sensing applications, as well as dynamic acceleration, resulting from motion, shock, or vibration.*

*The sensor is a polysilicon surface micromachined structure built on top of a silicon wafer. Polysilicon springs suspend the structure over the surface of the wafer and provide a resistance against acceleration forces. Deflection of the structure is measured using a differential capacitor that consists of independent fixed plates and plates attached to the moving mass. The fixed plates are driven by 180° out-of-phase square waves. Acceleration deflects the moving mass and unbalances the differential capacitor resulting in a sensor output whose amplitude is proportional to acceleration. Phase-sensitive demodulation techniques are then used to determine the magnitude and direction of the acceleration. The demodulator output is amplified and brought off-chip through a 32 kΩ resistor. The user then sets the signal bandwidth of the device by adding a capacitor. This filtering improves measurement resolution and helps prevent aliasing.*

*The ADXL327 uses a single structure for sensing the X, Y, and Z axes. As a result, the three axes sense directions are highly orthogonal with little cross-axis sensitivity. Mechanical misalignment of the sensor die to the package is the chief source of cross-axis sensitivity. Mechanical misalignment can, of course, be calibrated out at the system level.*

Source: Datasheet [3], page 10.

### **Communication interface**

The sensor has three analog outputs for each axis. The analog output can be filtered using external capacitors. For more details refer to chapter 6.

## Chapter 3

# Design-steps

Figure 3.1 represents the organizational timeline of the development.

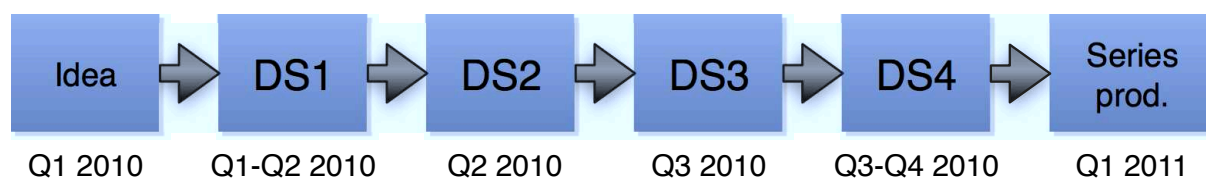


**Figure 3.1:** *Timeline overview*

### 3.1 Design-step 1 - proof of concept

DS 1 represents the first basic test of the possibility to develop a compass. The sensor is connected to the PC via the Infineon PGSI2 box.

#### 3.1.1 Basic proof of concept

The sensors hall\_ adc value is shown in a graph on the computer using MATLAB. Then the sensor was rised for about 1.5m and a change of the value when turning the sensor was recognizable.

#### 3.1.2 Extended proof of concept

Three sensors are mounted together and connected to the computer as shown in figure 3.4.



Figure 3.2: Picture of DS1



Figure 3.3: Scheme of DS1

## 3.2 Design-step 2

DS2 represents the first prototype. An overview of it is shown in Figure 3.6. An Arduino nano board (<http://www.arduino.cc/>) is used as main controller. Because of absence of

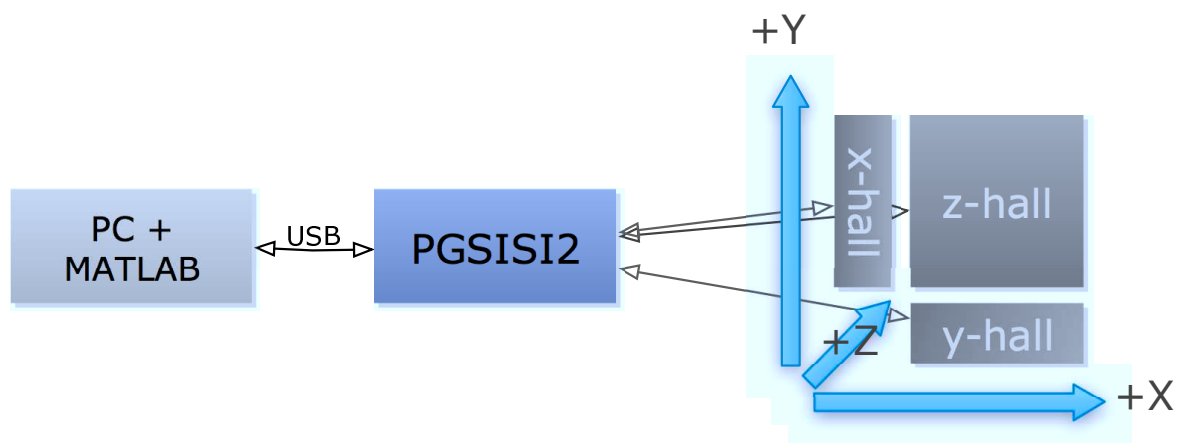


Figure 3.4: Scheme of extended possibility test

an accelerometer sensor, it is only built as a 2D compass.

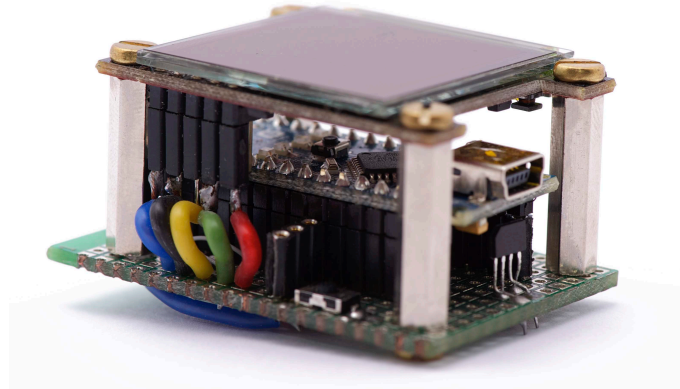


Figure 3.5: *Picture of DS2*

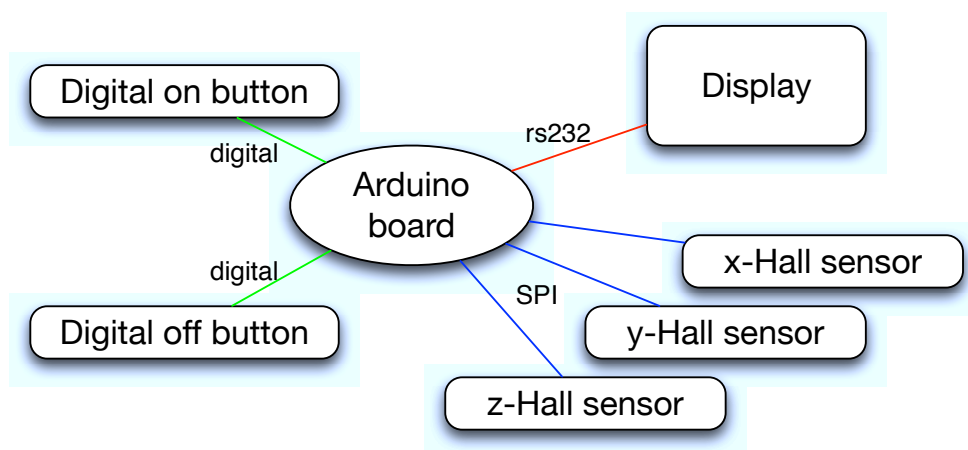


Figure 3.6: *Scheme of parts in DS2*

### 3.3 Design-step 3

DS3 packs all stuff of DS2 on a single pcb, adding an accelerometer for the 3D mode and a lithium-polymer battery for mobile usage.



Figure 3.7: *Picture of DS3*

### 3.4 Design-step 4

DS4 represents a release candidate of the compass (figure 3.8). Its main change is a thinner design to gain better mobility and an added battery charger. Later on also a case and a suitable packaging were added, but this is not part of the thesis. The front cover and picture of the packaging can be found in appendix C.

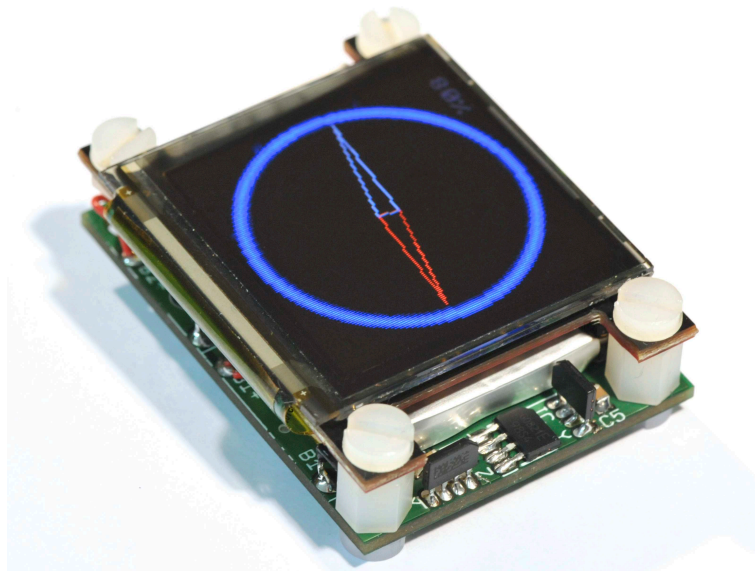
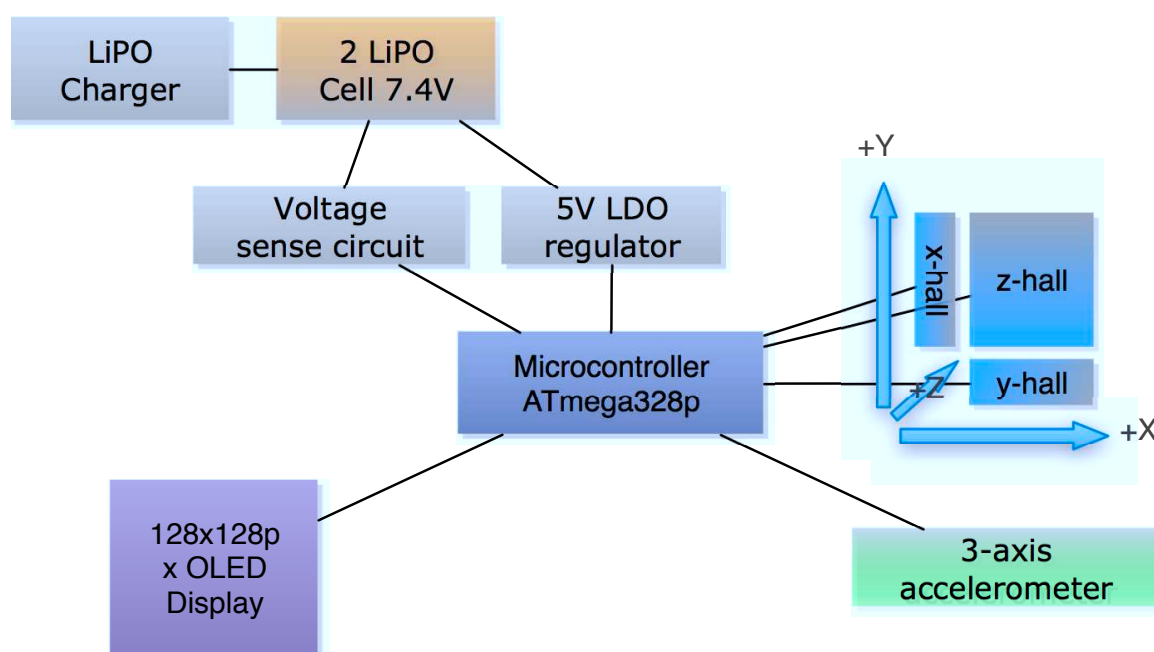


Figure 3.8: *Picture of DS4 without case*

## Chapter 4

# Hardware overview



**Figure 4.1:** *Hardware overview*

The hardware mainly consists of sensors, the display, micro-controller and the battery (+battery management).

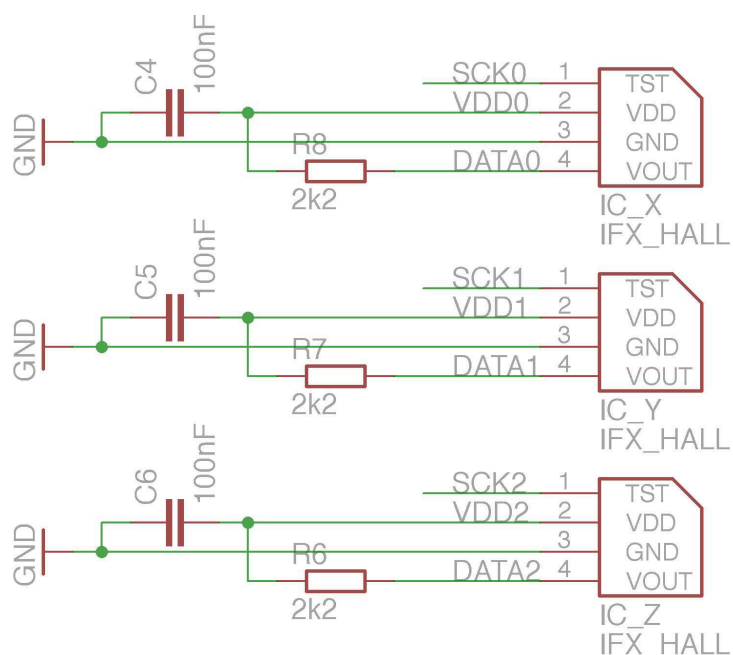
## 4.1 Sensors

A general part about the sensors is written in chapter 2. The mathematical part according to the magnetic field sensor is written in chapter 5 and about the accelerometer in

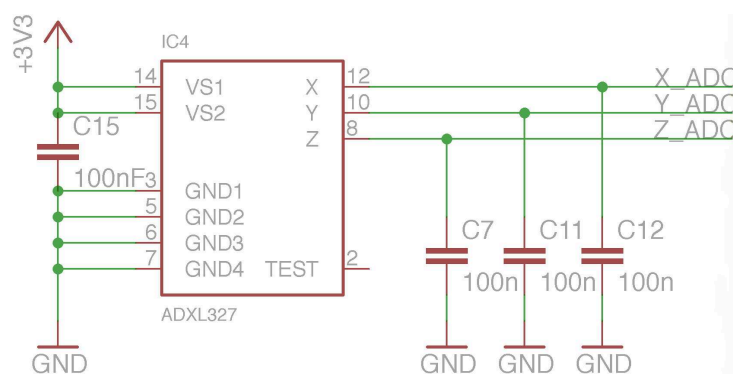
chapter 6.

Figure 4.2 shows the electrical connection of the hall sensors. Every sensor is supplied through an independent I/O of the microcontroller. This is possible because an I/O is able to handle a current of 20 mA and the sensor requires about 6 mA.

Figure 4.3 shows the electrical connection of the accelerometer.



**Figure 4.2:** *Electrical connection of the TLE4998 sensors*



**Figure 4.3:** *Electrical connection of the ADXL327 sensor*

## 4.2 Display

The display type is  $\mu$ OLED-128-G1h by 4D Systems <sup>1</sup>. Figure 4.4 shows a picture. It is based on the OLED technology to reduce the power drain. It is connected to the microcontroller directly via a serial interface. The display also offers a 3.3 V power output which is used to supply the accelerometer.

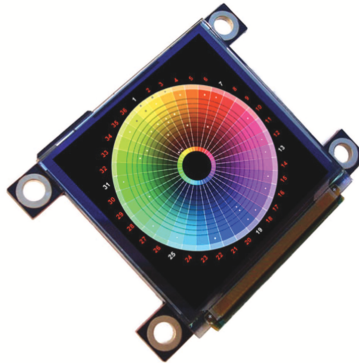


Figure 4.4:  $\mu$ OLED-128-G1h [1]

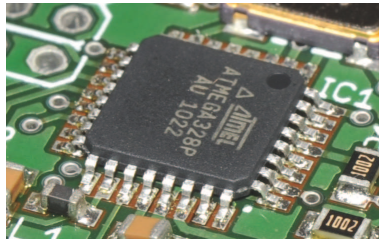
## 4.3 Microcontroller

Figure 4.5 shows a picture of the soldered microcontroller. The following table lists the most important specifications:

- Type: Atmel AVR ATmega328p
- Clock: 20 MHz
- Flash emory: 32 kB, 16 kB used
- SRAM: 2 kB
- ADC: 8 channel, 10bit
- Operating voltage: 1.8 – 5.5 V
- Operating current: 0.2 mA @1 MHz

---

<sup>1</sup><http://www.4dsystems.com.au/>



**Figure 4.5:** *Atmel ATmega328p microcontroller*

## 4.4 Battery

Two lithium-polymer batteries are used as power source. More information is available in chapter 8.

## Chapter 5

# Magnetic field data correction

### 5.1 The raw data

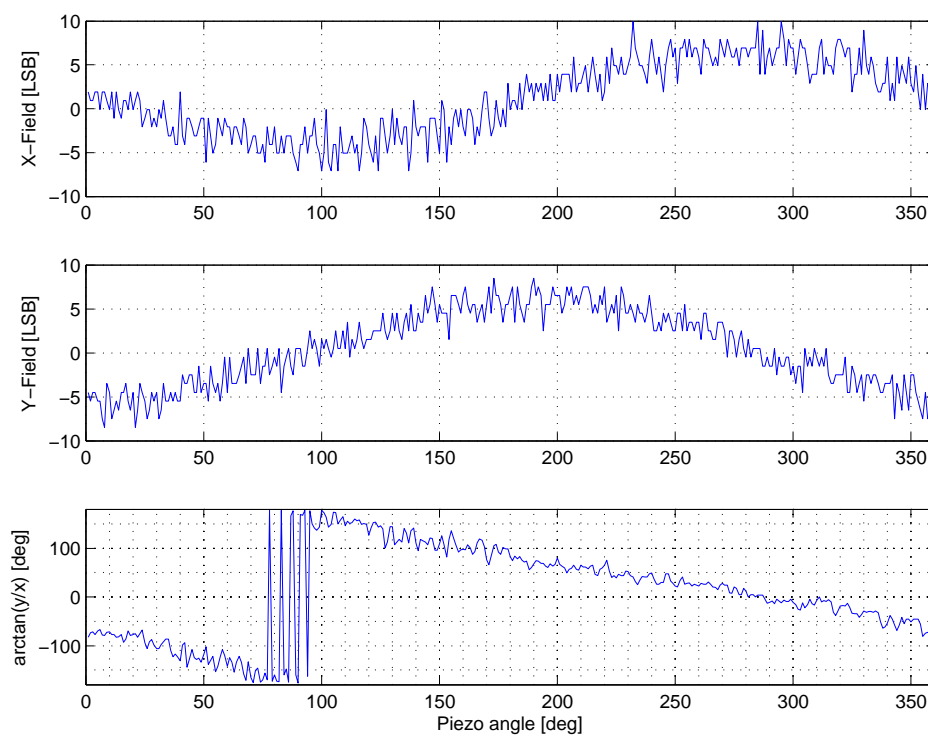


Figure 5.1: *360deg turn*

The sensors magnetic field range is set to 50mT, the earth magnetic field is only about 50μT. This means that the earth magnetic field is about  $\frac{50mT}{50\mu T} = 10.000$  times smaller than the sensors maximum field. The sensors resolution is 16bit. This results in a change of only  $\frac{65.535}{10.000} = 6.5LSB$  from the minimum to the maximum magnetic field. The raw data of the sensor is filtered by it's internal lowpass filter ( $f_{cutoff} = 80\text{ Hz}$ ,  $-3\text{ dB}$  point). Because the output data was still fluctuating, additional provisions have to be foreseen. Figure 5.1 shows the values of the x and y sensors during a 360deg turn using a piezo motor.

## 5.2 Filtering

The filter is designed using Matlabs *Filter Design & Analysis Tool* (fdatool). Equation 5.1 shows the transfer function of the digital filter. The parameters of the filter (set with the fdatool) are:

- Type: IIR, Lowpass, Butterworth, second order
- Sampling frequency  $F_s = 73Hz$
- Second order
- $F_{pass} = 0.2Hz$
- $F_{stop} = 1.5Hz$
- $A_{pass} = 1dB$
- $A_{stop} = 29dB$

Figure 5.2 also shows a screenshot of the fdatool.

$$G(z) = 0.00014582673611685 \cdot \frac{z^2 + 2z + 1}{z^2 - 1.965553879737854z + 0.966137170791626} \quad (5.1)$$

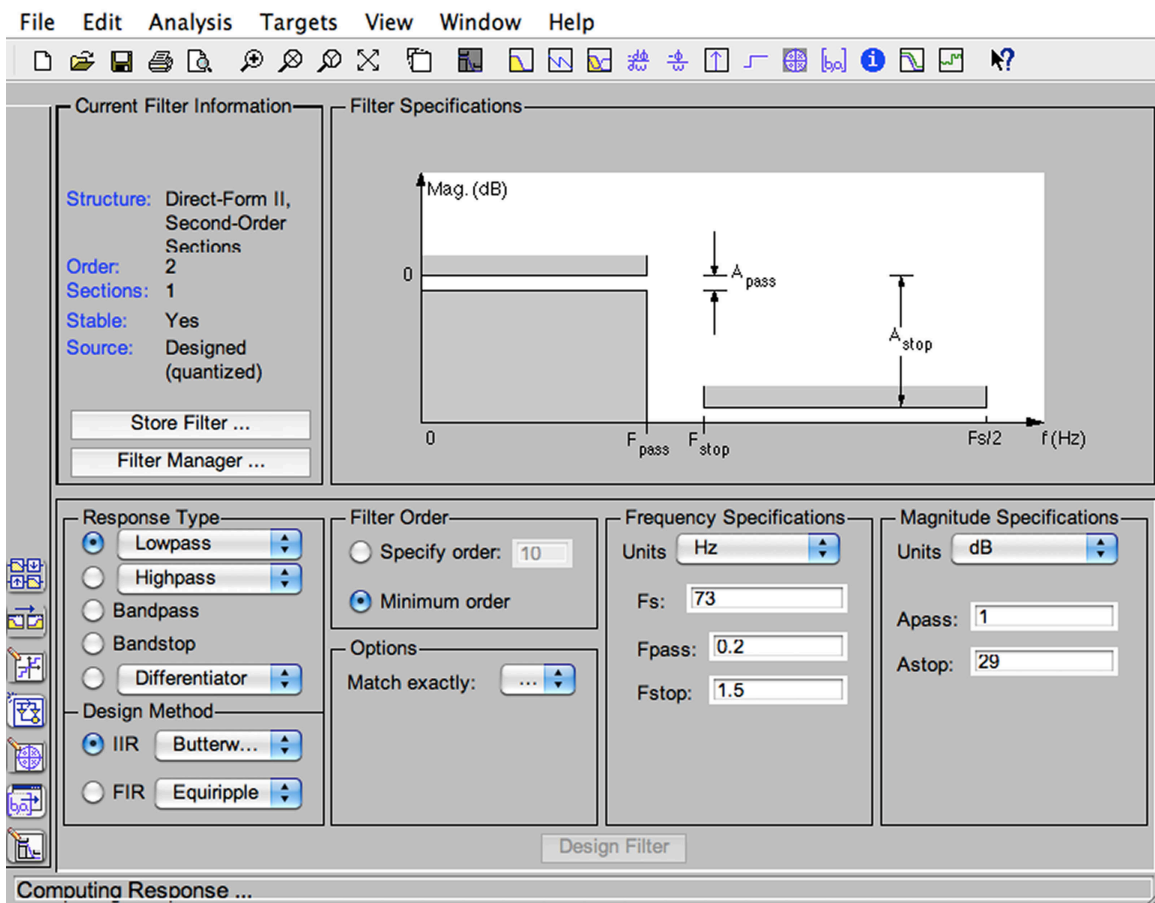


Figure 5.2: Screenshot of fdatool

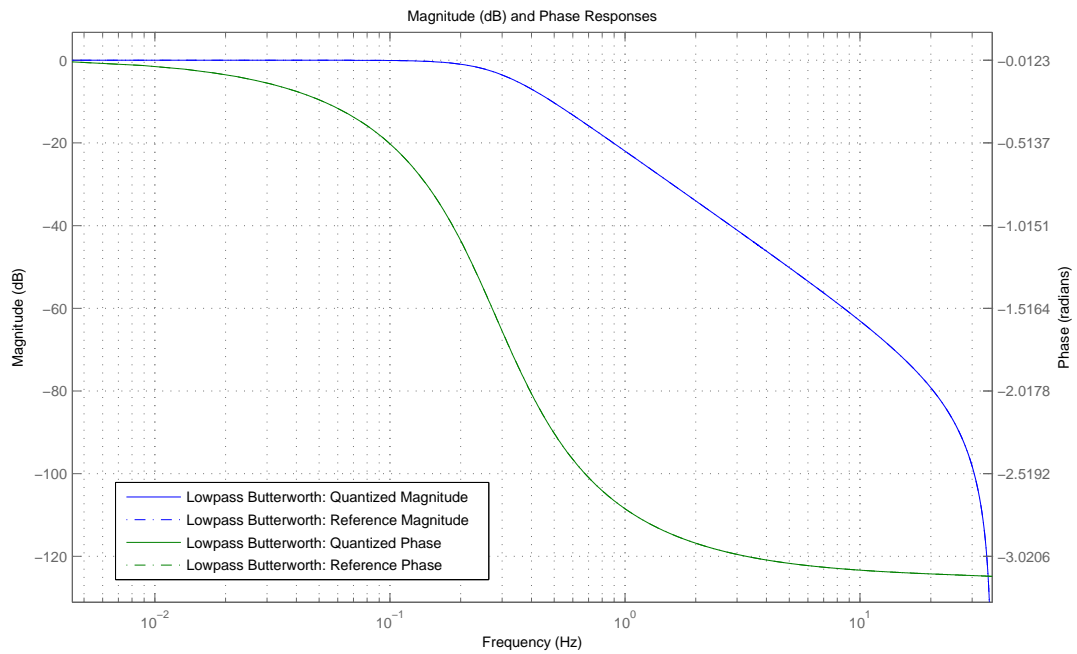


Figure 5.3: *Bode diagram*

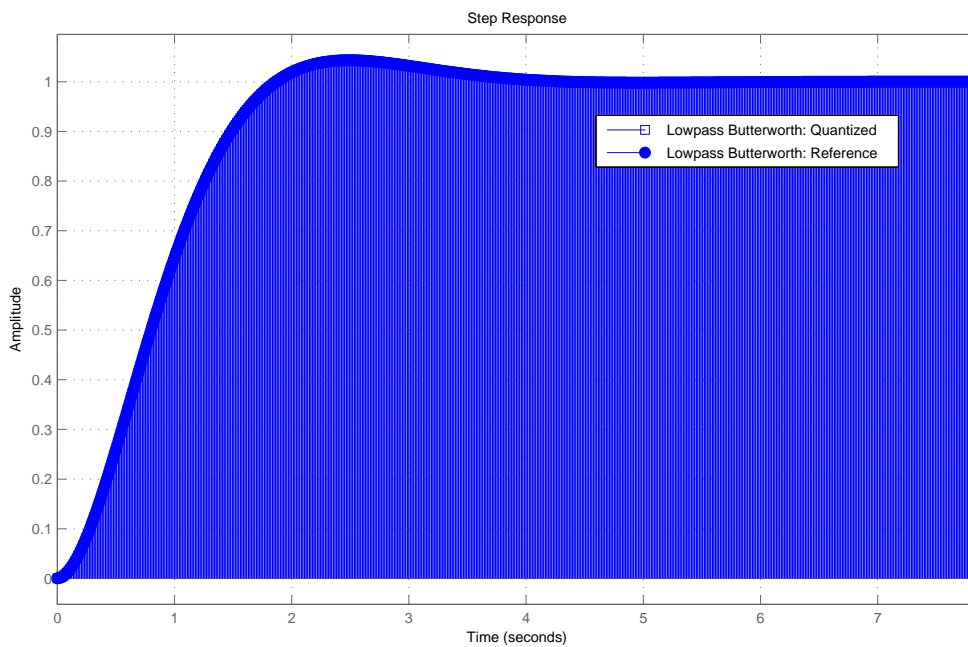


Figure 5.4: *Step response*

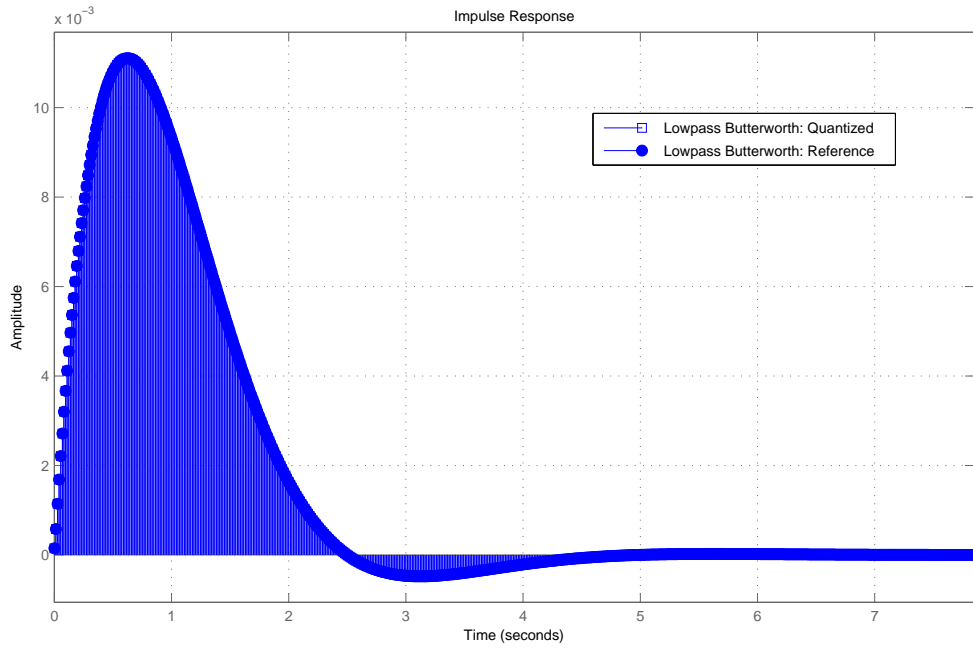


Figure 5.5: *Impulse response*

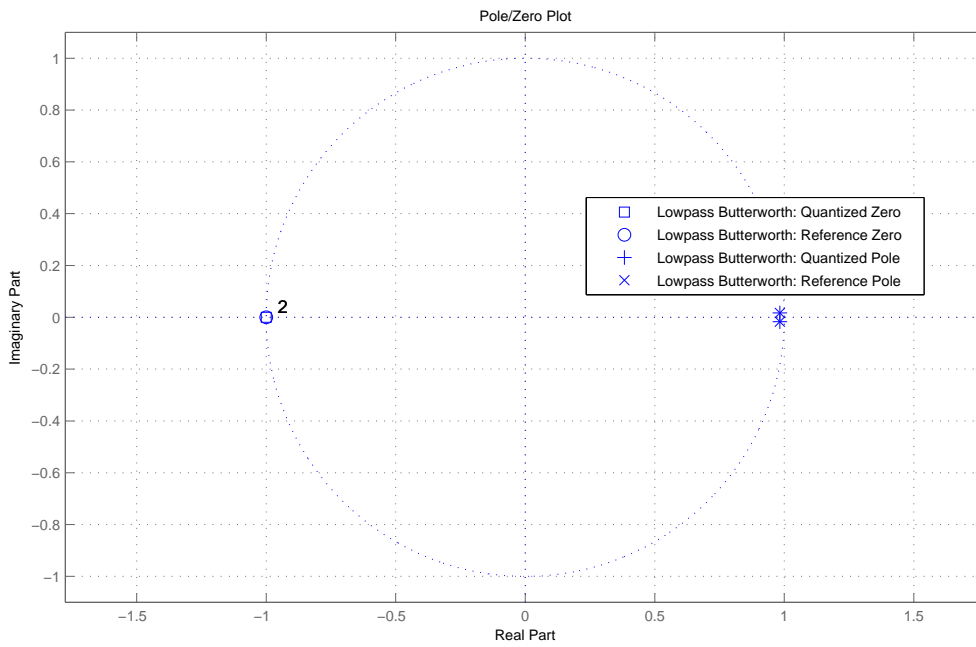


Figure 5.6: *Pole zero plot*

## 5.3 Calibration for offset correction

The hall-sensors inaccuracy is much higher than the earth magnetic field, so an offset correction has to be done. Equation 5.2 describes how the offset is calculated and subtracted of the raw, filtered sensor value.

$$\begin{pmatrix} x \\ y \\ z \end{pmatrix} = \begin{pmatrix} x_{raw} \\ y_{raw} \\ z_{raw} \end{pmatrix} - \frac{1}{2} \cdot \left[ \begin{pmatrix} x_{max} \\ y_{max} \\ z_{max} \end{pmatrix} - \begin{pmatrix} x_{min} \\ y_{min} \\ z_{min} \end{pmatrix} \right] \quad (5.2)$$

$x, y, z \dots$  current field

$x_{raw}, y_{raw}, z_{raw} \dots$  raw, filtered value of sensor

$x_{max}, y_{max}, z_{max} \dots$  highest measured value of sensor

$x_{min}, y_{min}, z_{min} \dots$  lowest measured value of sensor

The calibration process is started after the boot process of the compass. To calibrate, the minimum and maximum values have to be found. The text on the display, indicating that the compass is uncalibrated will disappear, as soon as each quadrant has been reached at least once. As soon as every quadrant has been reached more often (that means every quadrant has been hit for at least 3-5 seconds), the calibration will be classified as good and can not be disturbed again by external noise (eg. a magnet).

## Chapter 6

# Accelerometer data correction

## 6.1 Filtering

Accelerometer data is filtered twice. First filter is made up analog as described in the datasheet of the sensor [3] and the second one is a digital PT1 filter.

### 6.1.1 Analog lowpass filter

The analog lowpass filter is done as described in the datasheet [3] with a cutoff frequency of 50Hz. Figure 6.1 shows the bode diagram of the filter.

$$f_{cutoff} = \frac{1}{2\pi \cdot RC} = \frac{1}{2\pi \cdot 32 \text{ k}\Omega \cdot 100 \text{ nF}} = 50 \text{ Hz} \quad (6.1)$$

### 6.1.2 Digital lowpass filter

$$G(z) = 0.03698 \cdot \frac{z}{z - 0.9615} \quad (6.2)$$

The digital lowpass filter is used to remove errors caused by the analog-digital-conversion unit and to reach an even higher filtering effort. Figure 6.2 shows the bode diagram of this filter.

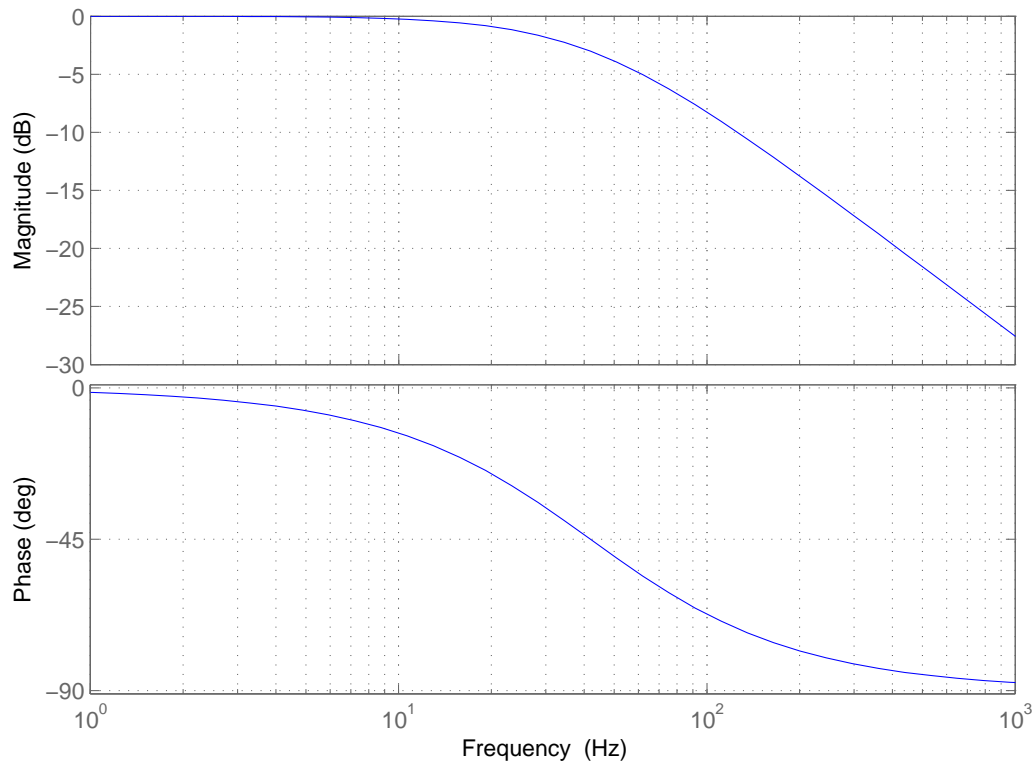


Figure 6.1: Bode diagram of the analogue filter for the accelerometer

## 6.2 Offset correction

No calibration is required to use the sensor. The minimum and maximum values are constants and were determined manually using the debug mode of the firmware.

$$\begin{pmatrix} x \\ y \\ z \end{pmatrix} = \begin{pmatrix} x_{raw} \\ y_{raw} \\ z_{raw} \end{pmatrix} - \frac{1}{2} \cdot (max - min) \quad (6.3)$$

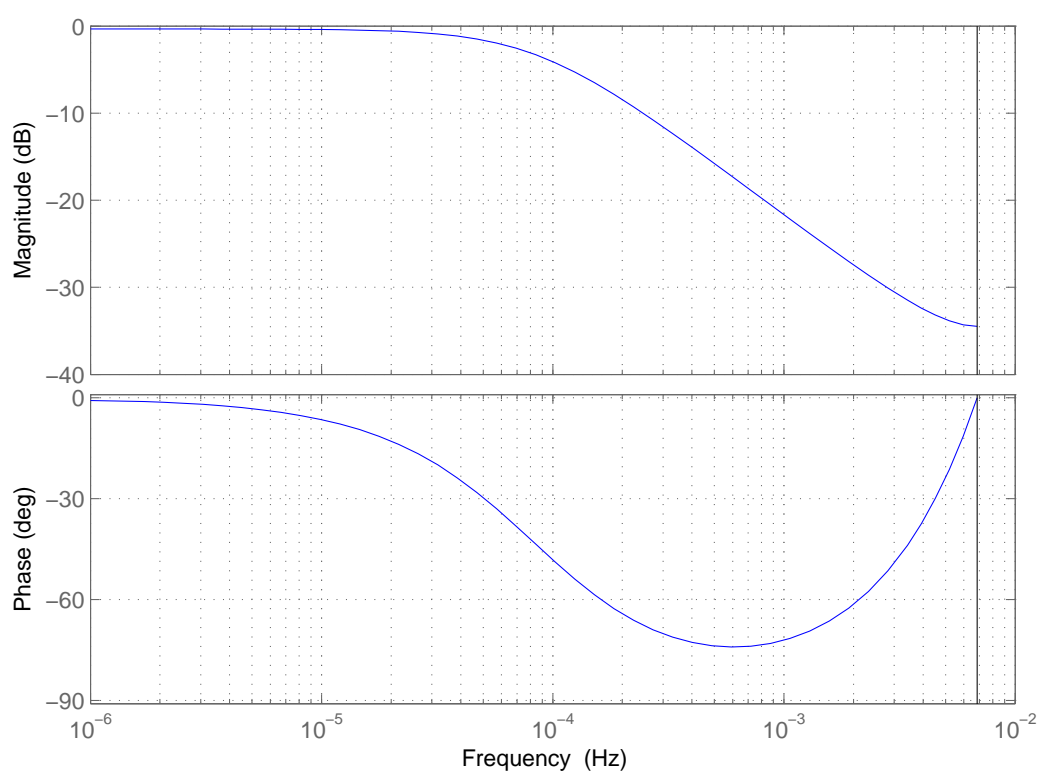


Figure 6.2: Bode diagram of the digital filter for the accelerometer

## Chapter 7

# Angle calculation

Figure 7.1 shows the arrangement of the three hall sensors.

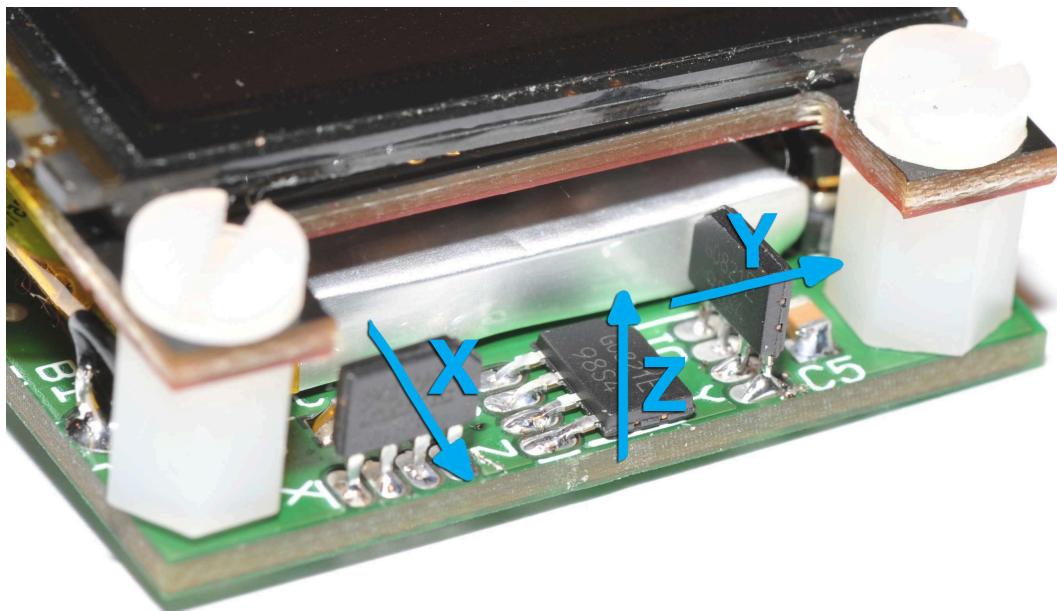


Figure 7.1: *Sensor arrangement*

## 7.1 Basic

For only 2D calculation of the angle, the simple equation 7.1 could be used.

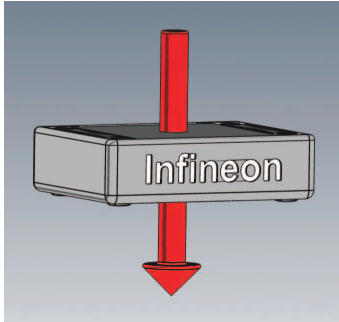
$$\alpha = \arctan \frac{y}{x} \quad (7.1)$$

## 7.2 3D calculation

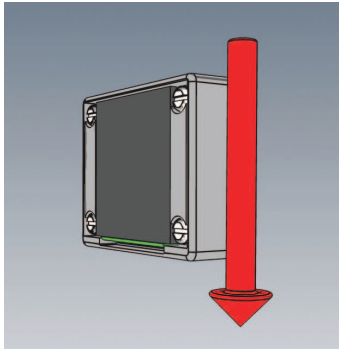
For 3D angle calculation, x and y in equation 7.1 has to be exchanged, according to the tilt of the compass (equation 7.2).

$$\alpha_{raw} = \arctan \frac{y \cdot |z_{acc}| + z \cdot y_{acc} + y \cdot |x_{acc}|}{-x \cdot z_{acc} + x \cdot |y_{acc}| - z \cdot x_{acc}} - offset \quad (7.2)$$

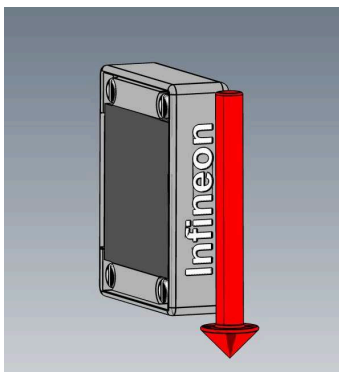
The following figures explain how this equation works. The blue part of the equation is the active one, that means the one, where the acceleration is high. Acceleration on the non-highlighted parts is nearly zero, so only the blue quotients are used for calculation of the angle. If the compass is tilted only a bit, the equation takes a part from both active situation to calculate the current angle.



$$\alpha_{raw} = \arctan \frac{y \cdot |z_{acc}| + z \cdot y_{acc} + y \cdot |x_{acc}|}{-x \cdot z_{acc} + x \cdot |y_{acc}| - z \cdot x_{acc}} - offset$$



$$\alpha_{raw} = \arctan \frac{y \cdot |z_{acc}| + z \cdot y_{acc} + y \cdot |x_{acc}|}{-x \cdot z_{acc} + x \cdot |y_{acc}| - z \cdot x_{acc}} - offset$$



$$\alpha_{raw} = \arctan \frac{y \cdot |z_{acc}| + z \cdot y_{acc} + y \cdot |x_{acc}|}{-x \cdot z_{acc} + x \cdot |y_{acc}| - z \cdot x_{acc}} - offset$$

## 7.3 Averaging

Averaging was not as easy as expected because it was necessary to average e.g. the two angles  $-170^\circ$  and  $+170^\circ$ . As an example,  $\frac{-170+170}{2} = 0$ , but the problem is that it should be  $180^\circ$ . Listing 7.1 shows the algorithm that solves the problem. It checks if the numeric difference between the old and new angle is bigger than  $180^\circ$ . If that occurs, it adds or subtracts  $360^\circ$  to the old angle to reach a numeric difference of lower than  $180^\circ$ .

**Listing 7.1:** *Angle averaging*

```
if ((rad[1] + M_PI) < rad_raw[0])
{
    rad[1] += 2.*M_PI;
}
else if ((rad[1] - M_PI) > rad_raw[0])
{
    rad[1] -= 2.*M_PI;
}

rad[0] = normalize_rad((rad_raw[0] + rad[1]) / 2.);
```

## Chapter 8

# Power management

## 8.1 Requirements

To keep a small device mobile, power has to be saved. Table 8.1 shows the power requirements of the important parts.

**Table 8.1:** *Power consumption*

| Pcs. | Part          | Voltage Range [V] | Current range [mA] | Current typ. [mA] |
|------|---------------|-------------------|--------------------|-------------------|
| 3    | TLE4998       | 4.5-5.5           | 3.0-8.0            | 12.0              |
| 1    | ADXL330       | 1.8-3.6           | 0.32               | 0.3               |
| 1    | uOLED-128-G1h | 4.0-5.5           | 12.0-120.0         | 45.0              |
| 1    | Atmega328p    | 1.8-5.5           | 1.0                | 1.0               |
|      |               |                   | Sum:               | 58.32             |

The power consumption of the uOLED-128-G1h (display) is variable. It depends on the displayed graphics. In comparison to ordinary LCD screens, OLED display do not make use of a backlight. Only non-black pixels are lit. This results in a very high contrast and very low power consumption. Measure with an ampmeter resulted a current drain of 60 mA.

## 8.2 Power supply

A 5V and 3.3V power supply had to be generated. The 3.3 V voltage is taken from the display as it generates 3.3V onboard for itself and provides it on pin 10 of it's connector [?].

The 5 V supply is generated by the very efficient LD2981 LDO voltage regulator. Another advantage of the LD2981 is the INHIBIT (=enable) pin. It can be used as digital switch so that the microcontroller is able to switch itself off.. Figure 8.1 shows the circuit of the voltage regulator. Device powering is done by a pressed button (S1\_ON), which pulls the INHIBIT pin high. The microcontroller starts executing and pulls the ENABLE line to high. After that the button can be released with voltage regulator in active mode.

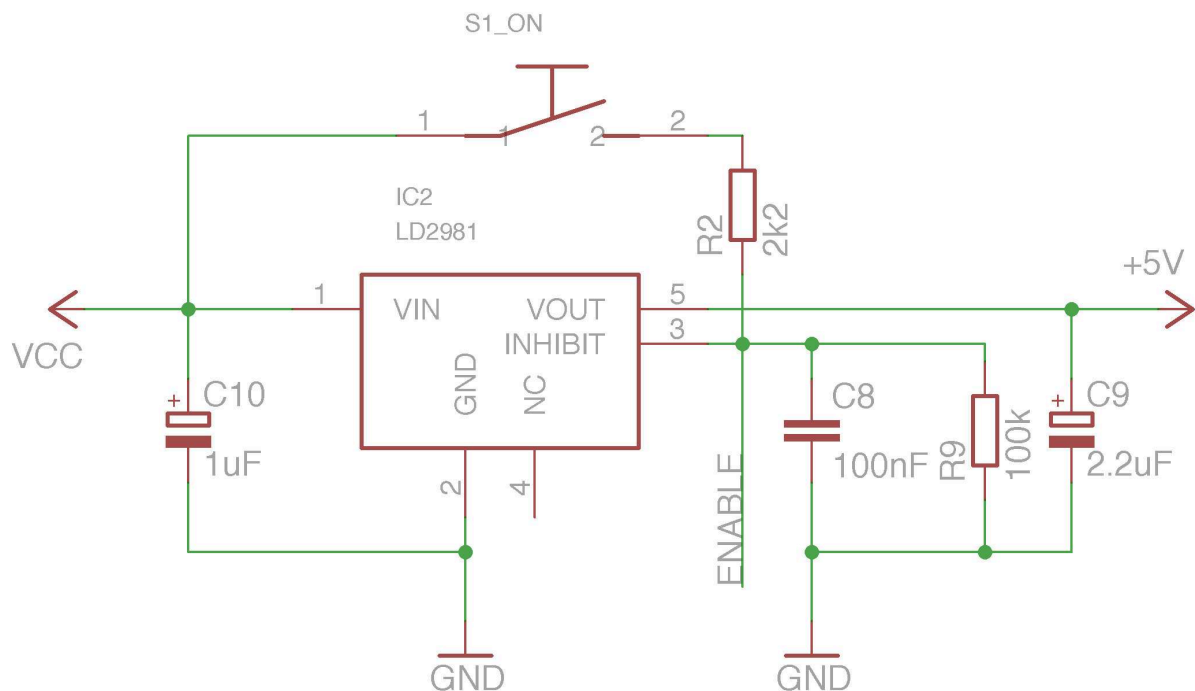


Figure 8.1: Voltage regulation

## 8.3 LiPO batteries

### 8.3.1 Overview

Lithium polymer batteries have a very high capacity. Today they are used in nearly every mobile phone, notebook and also in the newest electric and hybrid cars. One problem with these cells is a barely limited number of charge cycles. Today's cells are able to withstand about 300-1000 charge cycles. Many notebook manufacturers ship special software to extend the life cycle. This software stops the charging procedure at a set-able percentage (e.g. 90%). For the compass this is no problem because this number of charging cycles

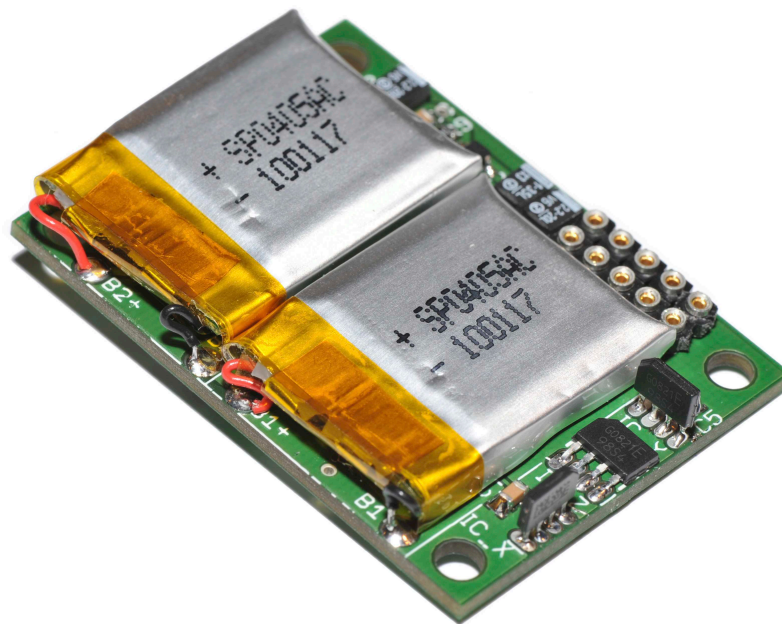


Figure 8.2: *LiPO batteries*

are not expected and necessary. Even a charge cycle per week will result in just 52 cycles a year (more than enough).

### 8.3.2 Charger

LiPO batteries need a special charging circuit. Figure 8.3 represents the schematics of the used charger. It gives a constant 140 mA current and constant 8.20 V voltage output. The idea of this schematic was copied from [2].

R12 sets the output current:  $R_{12} = \frac{0.6}{I_{max}} = \frac{0.6}{0.14} = 4.28 \Omega$

R11 sets the output voltage. It was first exchanged by a 2 k $\Omega$  potentiometer to find out the correct value for a 8.20 V voltage between B1- and B2+.

### 8.3.3 Protection

LiPO batteries have to be protected from overcharging ( $> 4.20$  V per cell, which would lead to an explosion) and deep discharge ( $< 2.9$  V per cell). Overcharging occurs by a voltage of 50 mV above 4.20 V. To prevent this, the charger stops charging at  $\sim 4.1$  V per cell (8.20 V on both installed cells). The two zener-diodes (D2, D4) are not intended to stop a charging cycle as they are too inaccurate. Their main purpose is to provide

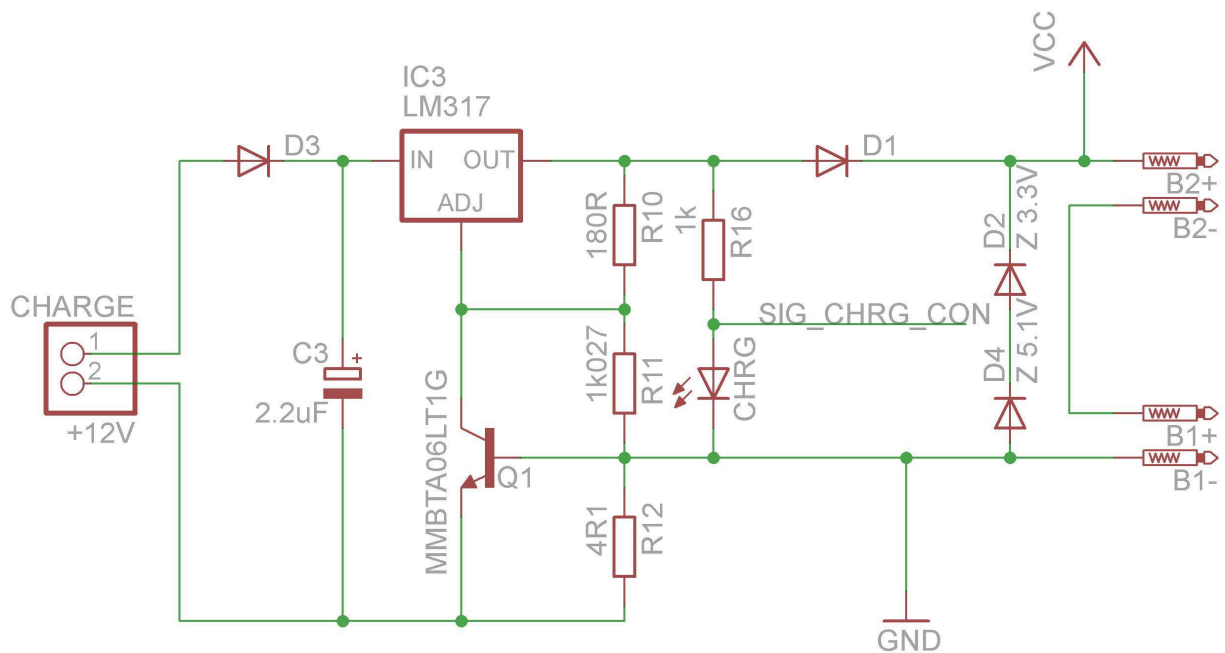


Figure 8.3: LiPO Charger circuit [2]

additional security on errors in the schematics. To prevent deep discharging, the compass is able to measure the battery voltage and to shut down itself at 3.1 V per cell. The cells are also internally protected from overvoltage, short circuit and deep discharge.

## 8.4 Battery voltage measurement

It's not possible to read the battery voltage directly with the ADC on the microcontroller. The reason is that the voltage is  $> 5$  V. To prevent this, a voltage divider of two resistors with the same size could be used. In this case the divider must not consume power when the compass is turned off to lower self-discharging of the batteries.

Figure 8.4 shows the circuit to switch off the power for the voltage divider / ADC when the compass is turned off (ie the ENABLE line is low). To reduce the power, Q2 is turned off by a pull-up resistor R15. If ENABLE goes high, Q3 turns on, pulls the base of Q2 to low and so the ADC is able to measure nearly half of the battery voltage between R4 and R5 (on the SUPPLY\_MEAS line).

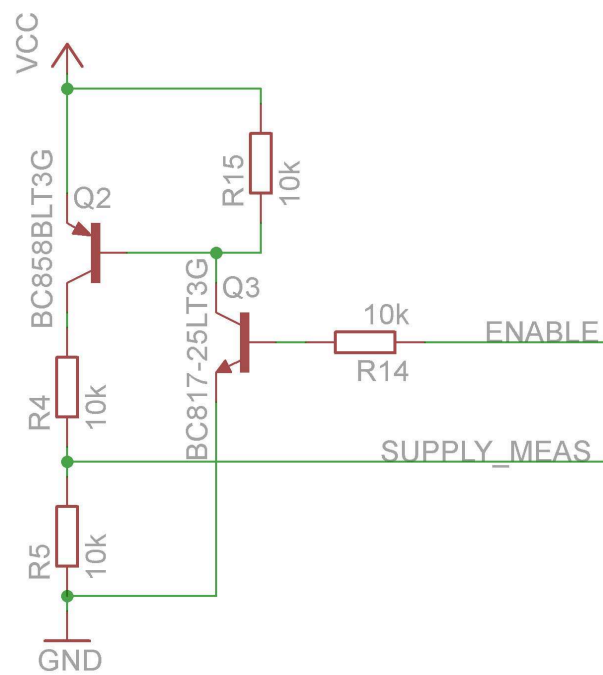


Figure 8.4: Battery voltage measurement

## Chapter 9

# Software structure

The firmware for the micro-controller is written in C and compiled using the `avr-gcc` compiler. The source is splitted in several files as it is shown in figure 9.1. The ADC files include lowlevel functions to read analogue voltages from the built-in ADC unit. The UART files include lowlevel functions to read and write serial data. This is mainly used to communicate with the display. The IFX-Hall-Sensor files implement functions for the digital communication with the TLE4998 hall sensors and the functions to code and encode the protocol. The OLED files implement many functions for drawing and writing stuff on the display. The EEPROM-Storage files offer a way for saving calibration data to the AVR internal EEPROM memory. In the last design-step this feature was deactivated as it offered no big advantage and caused a more complicated user interface. The angle conversions files include useful stuff for converting angles from radiant to degree and back, normalizing angles etc. The algorithm may be found in the file `main.c` and is summarized in figure 9.3. The file `main.h` includes constants and definitions for the project.

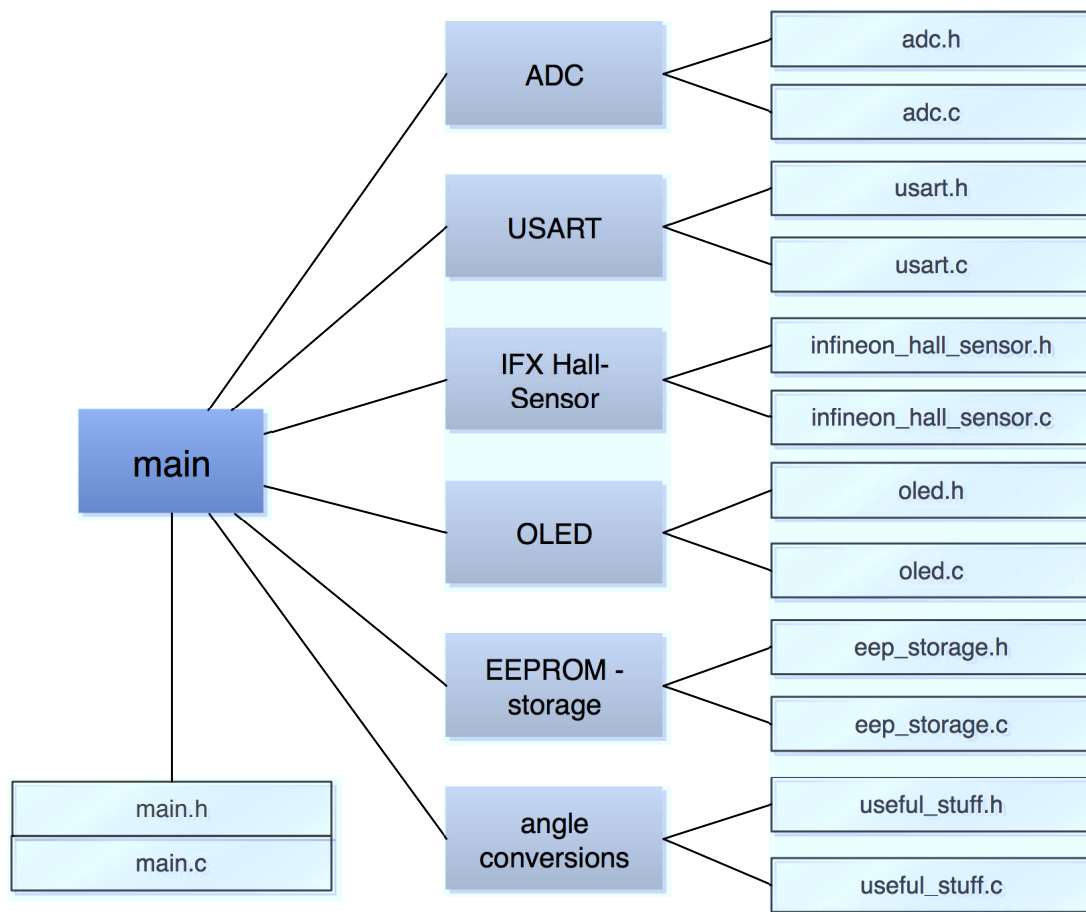


Figure 9.1: Software structure overview

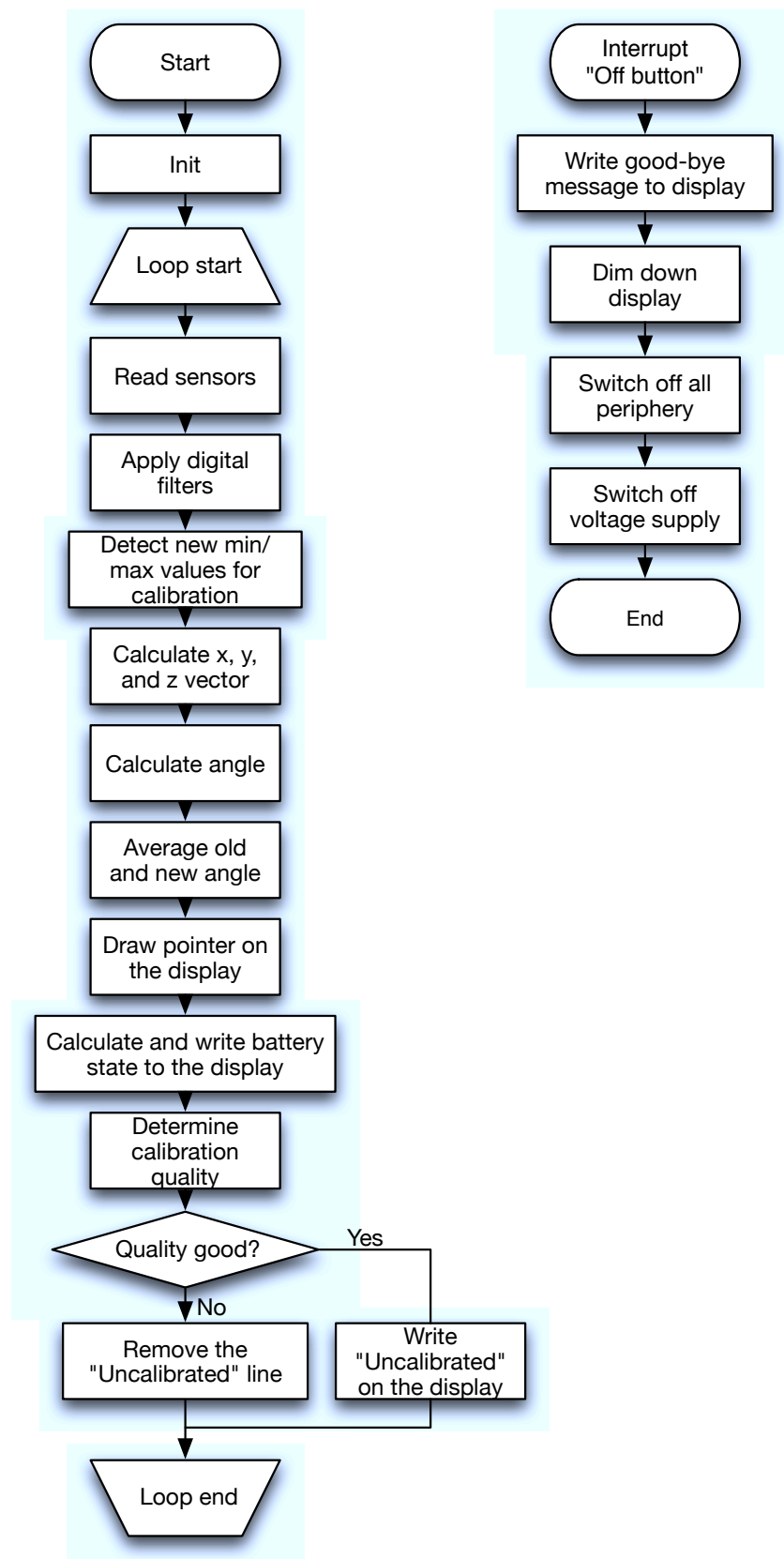


Figure 9.2: Simplified flowchart (page 1) of the main file

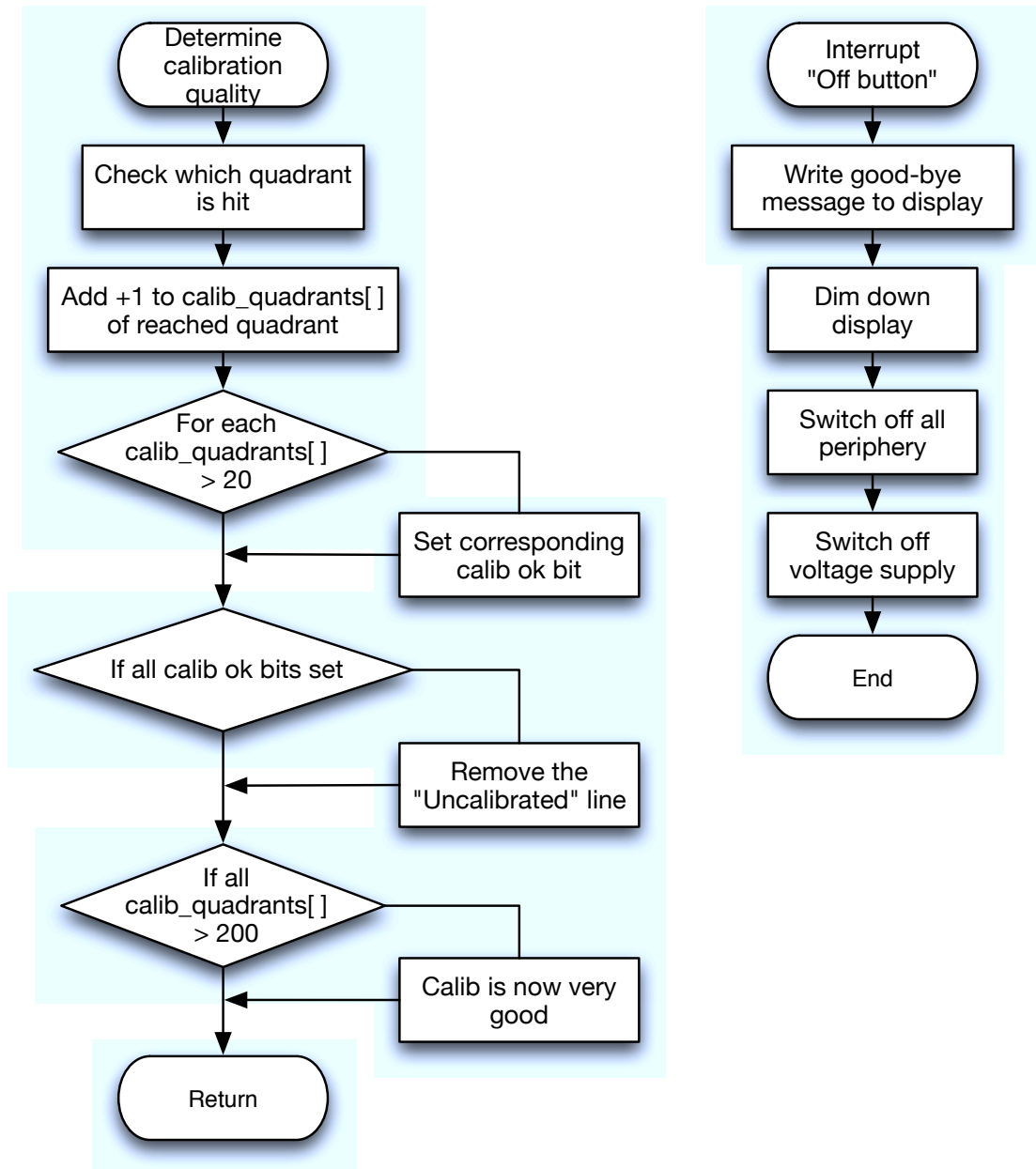


Figure 9.3: Simplified flowchart (page 2) of the main file

## Chapter 10

# Conclusion and outlook

Even through the sensors are of low resolution type, it is possible to measure small fields quite good using digital filters. It would be possible to improve the compass design by extending the update rate of the filters. This could be reached by eliminating the long delay time for display acknowledgement after update.

Furthermore it would be interesting to see if it is possible to exchange the hall-effect based sensor by a GMR-effect based angle sensor like the Infineon TLE5012. The TLE5012 already includes a GMR unit for sensing the X and Y direction. A 2D compass would be possible by just using only one sensor (instead of two independent TLE4998).

Another improvement could be done on the battery management. It would be a nice feature to monitor and control the charging voltage and current by software. This could extend the battery life dramatically.

# List of Tables

|                                 |    |
|---------------------------------|----|
| 8.1 Power consumption . . . . . | 28 |
|---------------------------------|----|

# List of Figures

|     |  |    |
|-----|--|----|
| 1.1 | Picture of the compass . . . . .   | 1  |
| 2.1 | Field lines on earth [7] . . . . .   | 2  |
| 2.2 | Magnetic sensor technologies' and their detection capabilities. The sensors are divided in three different groups of field ranges: lowfield (nT), Earth's field ( $\mu$ T), and bias field (mT). [9] . . . . . | 3  |
| 2.3 | Functional principle of a spinning hall element, [4] modified . . . . .  | 5  |
| 2.4 | Block diagram [5] . . . . .  | 5  |
| 2.5 | Photograph of the mounted acceleration sensor . . . . .  | 6  |
| 3.1 | Timeline overview . . . . .  | 8  |
| 3.2 | Picture of DS1 . . . . .   | 9  |
| 3.3 | Scheme of DS1 . . . . .  | 9  |
| 3.4 | Scheme of extended possibility test . . . . .  | 9  |
| 3.5 | Picture of DS2 . . . . .   | 10 |
| 3.6 | Scheme of parts in DS2 . . . . .   | 10 |
| 3.7 | Picture of DS3 . . . . .   | 11 |
| 3.8 | Picture of DS4 without case . . . . .  | 11 |
| 4.1 | Hardware overview . . . . .  | 12 |
| 4.2 | Electrical connection of the TLE4998 sensors . . . . .   | 13 |
| 4.3 | Electrical connection of the ADXL327 sensor . . . . .  | 13 |
| 4.4 | $\mu$ OLED-128-G1h [1] . . . . .   | 14 |
| 4.5 | Atmel ATmega328p microcontroller . . . . .   | 15 |

---

|     |   |    |
|-----|---|----|
| 5.1 | 360deg turn . . . . .   | 16 |
| 5.2 | Screenshot of fdatool . . . . .                                     | 18 |
| 5.3 | Bode diagram . . . . .  | 19 |
| 5.4 | Step response . . . . .   | 19 |
| 5.5 | Impulse response . . . . .  | 20 |
| 5.6 | Pole zero plot . . . . .  | 20 |
| 6.1 | Bode diagram of the analogue filter for the accelerometer . . . . . | 23 |
| 6.2 | Bode diagram of the digital filter for the accelerometer . . . . .  | 24 |
| 7.1 | Sensor arrangement . . . . .  | 25 |
| 8.1 | Voltage regulation . . . . .  | 29 |
| 8.2 | LiPO batteries . . . . .  | 30 |
| 8.3 | LiPO Charger circuit [2] . . . . .                                  | 31 |
| 8.4 | Battery voltage measurement . . . . .                               | 32 |
| 9.1 | Software structure overview . . . . .                               | 34 |
| 9.2 | Simplified flowchart (page 1) of the main file . . . . .            | 35 |
| 9.3 | Simplified flowchart (page 2) of the main file . . . . .            | 36 |
| A.1 | Full schematic page 1 . . . . .                                     | 44 |
| A.2 | Full schematic page 2 . . . . .                                     | 45 |
| B.1 | PCB layout . . . . .  | 47 |
| C.1 | Front cover . . . . .   | 49 |
| C.2 | Packaging . . . . .   | 50 |
| D.1 | User manual page 1 . . . . .  | 52 |
| D.2 | User manual page 2 . . . . .  | 53 |

# Nomenclature

ADC Analogue to digital converter

DSP Digital signal processor

fdatool Filter Design and Analysis Tool

IIR Infinite-impulse-response filter

LDO Low dropout regulator

LiPO Lithium-Polymer Battery

mA Milliamperes

OPA Operation amplifier

PGSISI2 Infineon Sensor Interface V2

T Tesla

UART Universal asynchronous receiver transmitter

# Bibliography

- [1] 4D SYSTEMS PTY. LTD. *uOLED-128-G1(SGC) User Manual*, 1.0 ed., 04 2008.
- [2] ADAMONE. Batteries for model aircraft. <http://adamone.rchomepage.com/guide3.htm>, 06 2010.
- [3] ANALOG DEVICES INC. *Small, Low Power, 3-Axis  $\pm 2$  g Accelerometer, ADXL327*, 0 ed. One Technology Way, P.O. Box 9106, Norwood, MA 02062-9106, U.S.A., 2009.
- [4] INFINEON TECHNOLOGIES, A. S. . C. Linear hall sensors. Internal, 2010.
- [5] INFINEON TECHNOLOGIES AG. *TLE4998S3/4 - Programmable Linear Hall Sensor*. Am Campeon 1-12, 85579 Neubiberg, Germany, 07 2008.
- [6] INFINEON TECHNOLOGIES AG. *TLE4998S/P-Programming Guide*. Am Campeon 1-12, 85579 Neubiberg, Germany, 02 2009.
- [7] LEWIS, D. There, in the water! a shark! a torpedo! a maggie? <http://lifeonshatsky.blogspot.com/2010/08/there-in-water-shark-torped>, 08 2010.
- [8] ©NERC, B. G. S. The earth's magnetic field: An overview. <http://www.geomag.bgs.ac.uk/education/earthmag.html>, 01 2011.
- [9] VANHA, R. S. Rotary switch and current monitor by hall-based microsystems. Master's thesis, ETH Zürich, 1991.

Appendix A

# Schematics

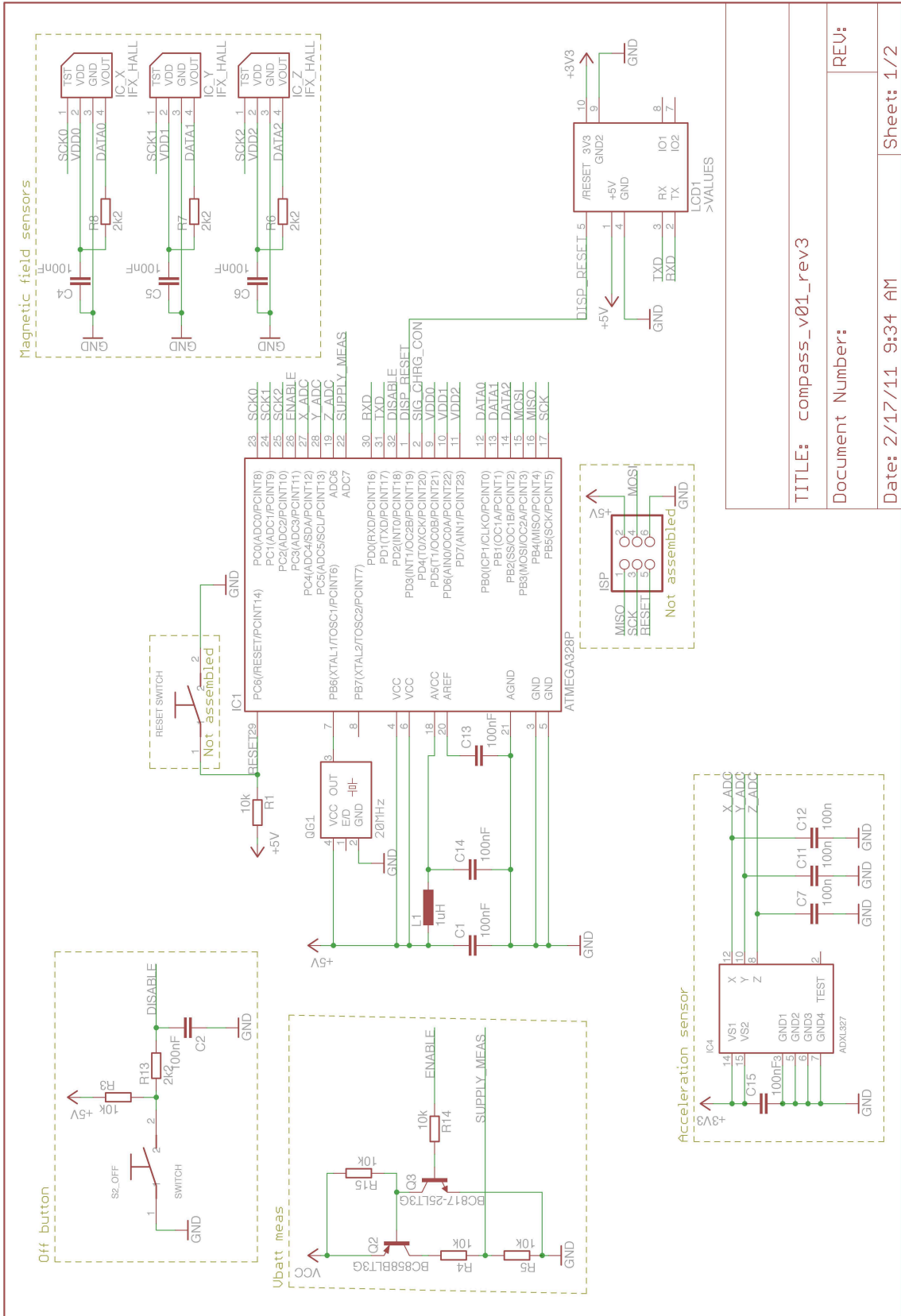


Figure A.1: Full schematic page 1

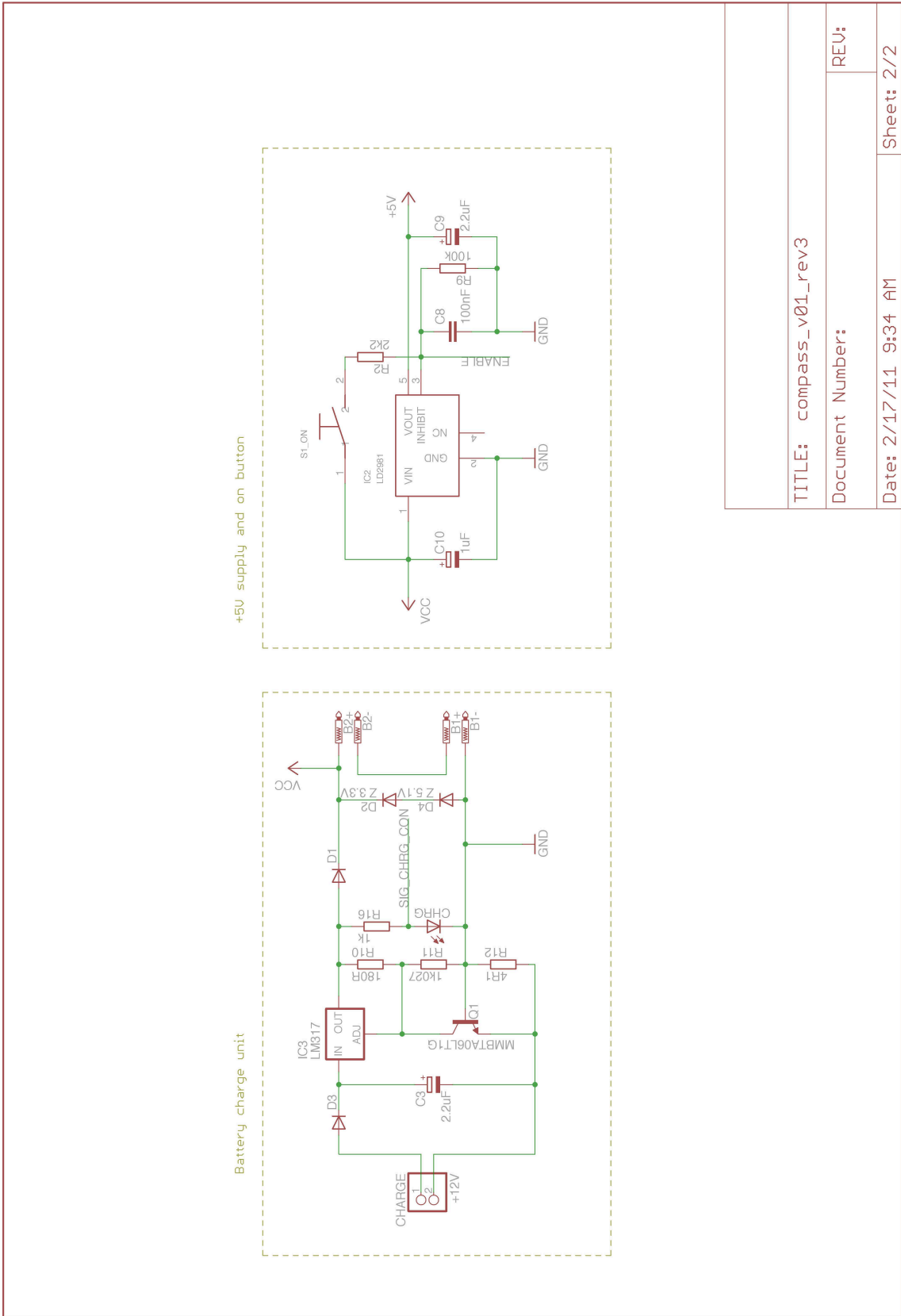
TITLE: compass\_v01\_rev3

Document Number:

REV:

Date: 2/17/11 9:34 AM

Sheet: 1/2



|                         |            |
|-------------------------|------------|
| TITLE: compass_v01_rev3 |            |
| Document Number:        | REV:       |
| Date: 2/17/11 9:34 AM   | Sheet: 2/2 |

Figure A.2: Full schematic page 2

## Appendix B

# PCB layout

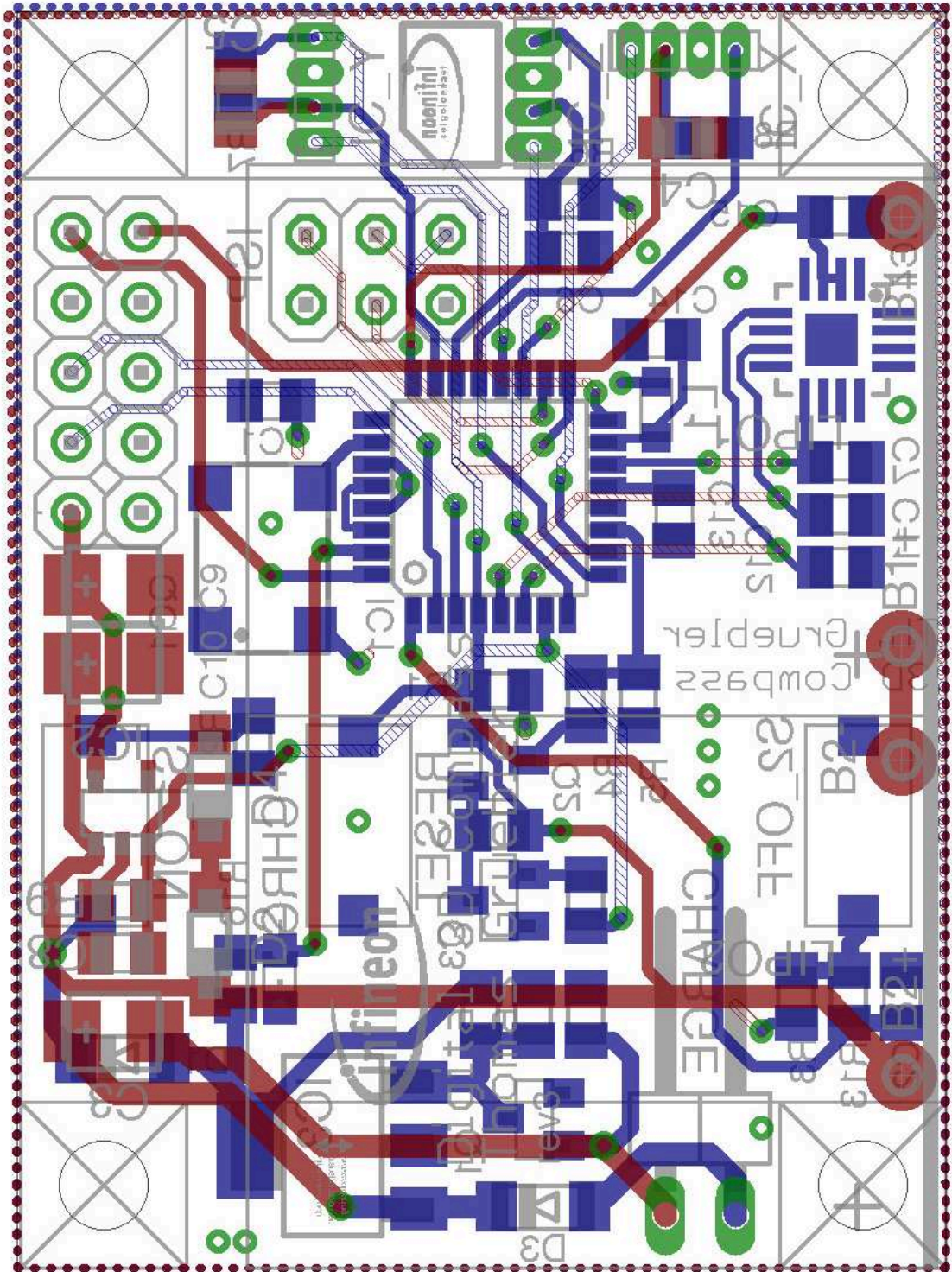
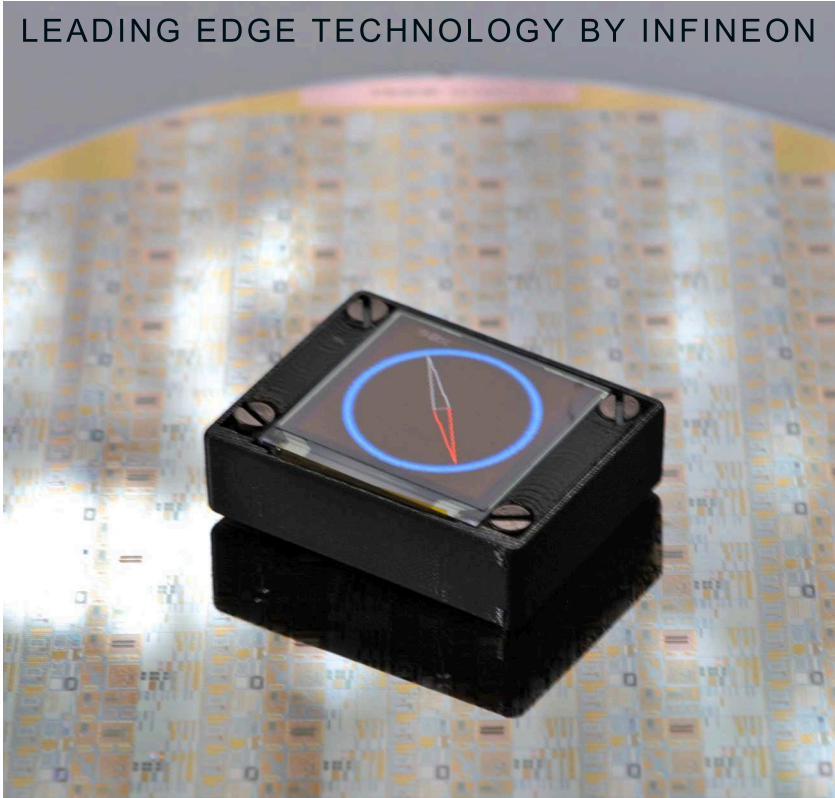


Figure B.1: *PCB layout*

Appendix C

# Packaging

LEADING EDGE TECHNOLOGY BY INFINEON



**Digital 3D Compass**  
Diploma thesis by Thomas Gruebler

Includes:

- Digital 3D Compass based on 3 TLE4998S4 hall-sensors
- 12 VDC Power plug
- User manual

Read manual before use!



Never stop thinking

Figure C.1: *Front cover*



Figure C.2: *Packaging*

Appendix D

User manual

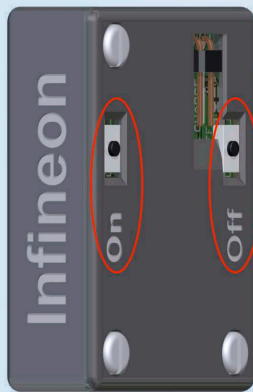


Figure D.1: User manual page 1

# Digital 3D Compass - User manual

## Buttons

The compass has two buttons on its bottom side:



## Switching on:

Press the "On" button for switching on. Never keep it pressed for longer than 1s!

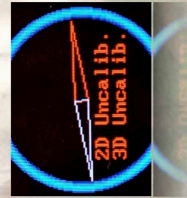
## Switching off:

Press the "Off" button for switching off.

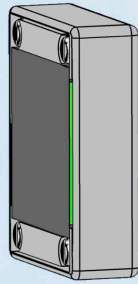
## Calibration

To calibrate the device, obey the following instructions:

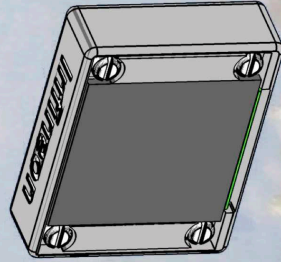
1. Turn the device around once.



2. Put the device on a flat surface where is no metal around. Slowly turn it around so that the pointer hits every quadrant of the compass and the "2D Uncalib." text disappears.



3. Put the compass on one of its sides. Turn it around as in step 2 until the "3D Uncalib." text disappears.



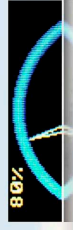
## Charging

In the upper left corner of the display you can see the current charging state in percent:



A red number indicates that the battery will get empty soon. In that case it's recommended to connect the charger as soon as possible.

An orange number indicates that the batteries are being charged.



A green number represents a fully charged battery.



To charge, connect the charging cable to the 2-pin connector on the bottom side of the compass. A blue light on the bottom will indicate a connected charger. If the blue light does not appear, change the polarity of the charger.



It is strongly recommended to switch off the compass during charging otherwise the batteries will not get fully charged.

Charging time: min 2h  
Average battery life: 2-3h

Figure D.2: User manual page 2

## Appendix E

# Sourcecode documentation

## Appendix F

# Datasheets